Japan Bilingual Publishing Co.

New Environmentally-Friendly Materials

http://ojs.bilpub.com/index.php/nefm

ARTICLE

Comparison of the Antibacterial Effect of Different Biological Silver Nanoparticles Synthetized and Integrated with Honeys

Victor Hugo Clébis[1] Sara Scandoriero[1] Wilma Aparecida Spinosa[2] Viviane Lopes Leite da Costa[2] Isabella Martins Lourenço[3] Amedea Barozzi Seabra[3] Renata Katsuko Katayama Kobayashi[1] Gerson Nakazato[1*]

1. Department of Microbiology, Center of Biological Sciences, Universidade Estadual de Londrina, Londrina, Paraná, CP 86057-970, Brazil
2. Department of Food Science and Technology, Center of Agrarian Sciences, Universidade Estadual de Londrina, Londrina, Paraná, CP 86057-970, Brazil
3. Center of Natural and Human Sciences, Universidade Federal do ABC, Santo André, São Paulo, CP 09210-580, Brazil

ARTICLE INFO

Article history
Received: 31 August 2022
Revised: 6 September 2022
Accepted: 8 October 2022
Published Online: 17 October 2022

Keywords:
Bee
Nanosilver
Green synthesis
Bactericidal
Honeys

ABSTRACT

This study compares the morphologies, zeta potentials, and antibacterial effects a total 12 different microcompounds containing honey and silver nanoparticles, in a novel study of the difference between honey samples in nanoparticle synthesis, as well as the antibacterial interaction that those honey samples can have with the silver nanoparticles synthetized using them. Microcompounds were synthetized by combining silver nitrate solution with a honey sample and performing one of methods of biogenic synthesis: sunlight exposure, basification to pH 5 or basification to pH 10. Samples of each microcompound were also submitted to heat treatment, obtaining thus heated variants. Morphology and size data were obtained by Dynamic Light Scattering (DLS) analysis and Scanning Electron Microscopy (SEM); while zeta potential was measured by Electrophoretic Light Scattering. Broth microdilution, time-kill curves and SEM were used to access the antibacterial effect. Mean diameter of particles inside all microcompounds varied between 100 nm and 150 nm; and the zeta potential varied depending on the honey used. Minimal Inhibitory Concentrations (MIC) of microcompounds were between 15 μM and 500 μM. Time-kill curves showed that microcompounds had a faster and stronger effect against *Escherichia coli* than *Staphylococcus aureus*. Microcompounds obtained by basification to pH 5 or by sunlight were bactericidal, as they were capable of inhibiting bacterial growth (resulting in an antibacterial efficiency of 100% in 24 hours) at 125 μM against *S. aureus* and 62.5 μM against *E. coli*. SEM micrographs showed bacterial cells with lower cell density, blebs and other alteration after microcompound treatment.

*Corresponding Author:
Gerson Nakazato,
Department of Microbiology, Center of Biological Sciences, Universidade Estadual de Londrina, Londrina, Paraná, CP 86057-970, Brazil;
Email: gnakazato@uel.br; gersonakazato@yahoo.com.br

DOI: 10.55121/nefm.v1i1.46

1. Introduction

According to the World Health Organization (WHO) [1], infections caused by resistant bacteria take 700,000 lives yearly. The selection of resistant bacteria occurs naturally due to the prescription of antibacterial substances; however, the misuse of antibiotics and their inappropriate disposal accelerate the process [1]. Antimicrobial resistance to available drugs is detected in 35 percent of common human infections in countries participating in the Organization for Economic Co-operation and Development (OECD). Additionally, low and middle-income countries present 80 to 90% resistance rates for treatment-bacterium combinations, which led to WHO compiling a list of antibiotic-bacterium combinations that require an alternative [2,3]. Thus, many organizations have established the necessity for developing new antibacterial treatments, including "remodelling" old treatments [1,4,5].

Since ancient times, civilizations have used metals like silver (Ag), copper, and zinc against infections, with silver being considered the most popular and employed in procedures involving dental care, burns, and wounds [6-11]. However, in order to circumvent possible adverse effects, studies have processed metals into microcompounds, which grants them additional antibacterial mechanisms [7-11].

Due to their positive surface charge, most nanoparticles can interact with the negatively charged structures. Target examples include phosphates and carboxylates present in the external wall of Gram-negative bacteria, and teichoic acid in Gram-positive bacteria [12-15]. Once inside, they can display multiple antibacterial mechanisms, depending on their morphology, interact with the bacterial membrane and intracellular components such ribosome and bacterial chromosomes, causing oxidative stress and disrupting the bacterial cell's electronic balance, and reach an antibacterial efficacy of 100% [9,11,14-16]. These properties grant metal nanoparticles a more selective antibacterial compared to colloidal silver, enabling their clinical use [11,17].

Several nanoparticle synthesis and modulation methods use honey as a reducing and stabilizing agent, as its oxygen peroxide and glucose can reduce metallic ions, while its gluconic acid and proteins stabilize the particles formed [18-24]. Those molecules nanoparticles can be synthesized at room temperature through basification and electron excitation by sunlight [20,22,25-28]. However, nanoparticle core size, shape, and content may vary per synthesis protocol used, silver concentration, and honey composition [18-20].

Honey samples can present varying physicochemical thus antibacterial properties, according to geographical and botanical origins, soil composition, producing bee, and harvest season [29-34]. Notably, the reducing sugars and oxygen peroxide can vary significantly samples. For example, honey produced by *Scaptotrigona bipunctata* (shown to contain a relevant antibacterial potential) has lower sugar content and greater humidity than the conventional honey produced by *Apis mellifera* [31,34-36]. Therefore, usage of a different honey sample may alter silver particles' structure as well as their antibacterial property.

Additionally, honey contains antibacterial properties, which can further enhance the antibacterial potential of nanoparticles. For example, the hydrogen peroxide causes oxidative stress in bacteria, and flavonoids exhibit antioxidative, antiviral, and anticancer properties [29,30,35-38]. Furthermore, Manuka honey, produced by *A. mellifera* collecting nectar from the *Leptospermum ssp.* trees; is used in products such as the Medihoney® Antibacterial Wound Gel for professional wound care, which is an example of honey's potential in the clinical use of nanoparticles [29,39,40].

In light of the antibacterial effects of honey and silver nanoparticles, we decided in a novel study to compare the nanoparticles synthesis using two honey samples with contrasting compositions. We intend to assess how the differences in honey composition can affect the morphology and antibacterial effect of the resulting silver nanoparticles, as well as observe the antibacterial interaction those honey samples can have with the particles.

Thusly, we developed and compared different microcompounds made with silver and honey with two honey samples – a honey sample collected from *Apis mellifera* (nominated Honey *Apis mellifera*- "HAM") and another one collected from *Scaptotrigona bipunctata* (nominated honey Scaptotrigona bipunctata- "HSB"). Microcompound synthesis used three different methods for nanoparticle formation: basification, sunlight exposure, and aggregative basification. After synthesis, post-heating of microcompound samplings resulted in different morphological and antibacterial properties. The resulting twelve types of microcompounds are compared in this work in relation to their particle size and antibacterial properties, through Dynamic Light Scattering (DLS) measurement and antibacterial assays, respectively, in order to assess their clinical potential; in addition, this article presents and analyses micrographs of microcompounds and bacteria obtained by Scanning Electronic Microscopy (SEM).

2. Materials and Methods

2.1 Honey Harvesting and Composition Analysis

The HAM and HSB samples originated from the university meliponary (Universidade Estadual de Londrina, Londrina-PR, Brazil) and the Unidade de Conservação Monte Sinai (Mauá da Serra-PR, Brazil). They were col-

lected between 2018 and 2019 with glass syringes and metal spatulas; and deposited in sterilized jars for transport. HAM honey was harvested from Africanized *A. mellifera* Latreille (Hymenoptera: Apidae) hives, and HSB was collected from *S. bipunctata* Lepeletier 1836 (Hymenoptera: Apidae: Meliponinae) nests. Both have unifloral *Eucalyptus sp.* as their botanical origin.

Comparison of HAM and HSB composition, color, humidity, ash content, pH, total HAM and HSB composition, color, humidity, ash content, pH, total acidity, and sugar content comparison followed standards and protocols well established by the Association of Official Analytical Chemists International (AOAC International) in 2019 [41]. The color analysis used a Lovibond instrument, the humidity measurement, a digital refractometer (AOAC 969.38 method). The ash content was weighted by heating in an industrial oven at 600 °C for four days (AOAC 920.181 method). The honey pH, lactones, and total acidity were determined by titration of samples with a 0.1 M NaOH solution (Sigma-Aldrich® Brazil) to a pH value of 8.3 and 10 (AOAC 962.19 method). The reducing and total sugars were analyzed by apparent reducing sugar (AOAC 920.183 method), based on the reduction of copper hydroxide in Fehling's solution. All tests occurred in the Food Analysis Laboratory of the State University of Londrina, using non-sterilized HSB and HAM samples. Before microcompound formation, both HAM and HSB were diluted in water (50% $v \cdot v^{-1}$), sterilized by filtration using a 0.22 µm filter (Millipore®), and stored at 4 °C.

2.2 Methods of Biogenic Microcompound Synthesis and Measurement by DLS and SEM

Microcompounds were obtained by varying three factors in their synthesis: the chosen honey sample, the mechanism of nanoparticle synthesis, and heating after the nanoparticle formation. The methods used for synthesis in this study followed data and protocols from articles published by González et al. (2016) [20], Priz (2014) [42], and Tagad et al. (2013) [43].

Three prepared samples of "HAM" and "HSB", each at 50% ($v \cdot v^{-1}$), were mixed (50% $v \cdot v^{-1}$) with a solution of 5 mM of $AgNO_3$ (Sigma-Aldrich®, Brazil); and afterward, each solution underwent one of the three methods for biogenic particle synthesis selected. As shown in Table 1, solutions containing the microcompounds' substrates were either exposed to sunlight for 10 min; or basified by adding a 1 M NaOH solution (Sigma-Aldrich® Brazil) until the solution to pH 5.0 or 10.0. All solutions were mixed and left at room temperature for 5 min before storage at 4 °C for 24 h. Samples from each microcompound were then collected and heated separately at 60 °C for 30 min by water bath, and stored at 4 °C before performing the assays described below. The total number of microcompounds tested were twelve. The nomenclature of microcompound type shows its constituent honey, the method used in its synthesis, and whether the microcompound underwent heat treatment as schematized in Figure 1 and shown in Table 1.

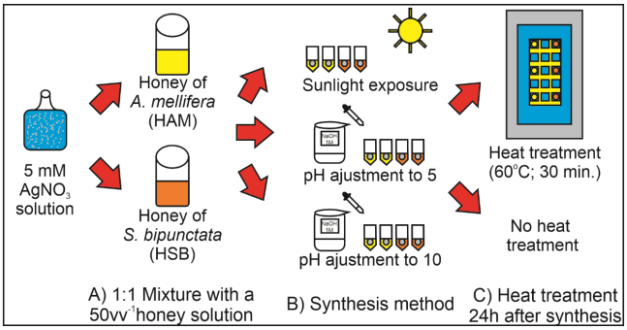

Figure 1. Schematic representation of synthesized microcompound types using honey collected from *Apis mellifera* honeybees (HAM) or honey collected from *Scaptotrigona bipunctata* stingless bees (HSB).

Source: Own authors.

Table 1. Types of microcompounds obtained and their nomenclature.

Honey sample used	Synthesis method	Heating	Type of microcompound
Africanized *A. mellifera* Latreille "HAM"	Sunlight exposure	Yes	HAM L
		No	HAM Lδ
	Basification (pH 5.0)	Yes	HAM pH 5
		No	HAM pH 5δ
	Aggregative basification (pH 10.0)	Yes	HAM pH 10
		No	HAM pH 10δ
S. bipunctata Lepeletier 1836 "HSB"	Sunlight exposure	Yes	HSB L
		No	HSB Lδ
	Basification (pH 5.0)	Yes	HSB pH 5
		No	HSB pH 5δ
	Aggregative basification (pH 10.0)	Yes	HSB pH 10
		No	HSB pH 10δ

Microcompound diameter was determined through dynamic light scattering (DLS) analysis with photon correlation spectroscopy (ZetaSizer NanoZS, Malvern® Brazil). Zeta potential was determined by electrophoretic mobility inspection of surface charges using the same equipment. Readings for all microcompounds were made in triplicate. Microcompounds in the solutions obtained from the synthesis were washed through centrifugation of 1 mL collected from each sample for 1 h at 24 °C and 31,340.00 g. The resulting pellets were resuspended in 1 mL of deionized

water inside microtubes, obtaining thus washed microcompounds. Silver particles inside the microcompounds were assessed through atomic absorption spectroscopy at 400 nm (AAnalyst 700, Perkin Elmer, USA) and compared to reference standard solutions (Specsol, Brazil).

Aliquots of 10 µL from the microtubes containing the washed silver particles were pipetted on polylysine-coated (1%) glass slides. Those were fixed after drying by immersion in a sodium 0.1 M cacodylate buffer solution (pH 7.2) containing 2% glutaraldehyde and 2% paraformaldehyde for 20 h; and then post-fixed in 1% OsO4 for 2 h. The fixed slides were submitted to progressive dehydration by submersion in increasing ethanol gradients (70, 80, 90, and 100 °GL). Next, samples were critical point-dried using CO_2 (BALTEC CPD 030 Critical Point Dryer), coated with gold (BALTEC SDC 050 SputterCoater). Lastly, the prepared slides were observed with a scanning electron microscope (FEI Quanta 200), and pictures were taken at 20,000×. The diameter of equivalent circle, roundness, and circularity of particles within the microcompounds were analyzed using the ImageJ photoshop software.

2.3 Microdilution Assays of Washed Microcompounds

Minimal Inhibitory Concentrations (MIC) of each type of washed microcompound were evaluated following the Clinical and Laboratory Standards Institute (CLSI, 2018) [45] guidelines for serial dilution in 96-well plates. A bacterial strain was cultivated in Mueller-Hinton (MH) broth (Difco®) agar for 24 hours before the assay, and then, suspended in a sterile saline solution (NaCl 0.85%, Sigma-Aldrich® Brazil) at 1.5×10^8 CFU·mL^{-1} (0.5 on the McFarland scale); from which 10 µL were transferred to microtubes containing 990 µL MH (Difco®) broth. From those microtubes, aliquots containing 50 µL were pipetted in wells containing 50 µL of a microcompound solution, obtained by serial dilution of a given type of microcompound in MH (Difco®) broth. The final concentration of bacterial cells was 5.0×10^5 Colony Forming Units (CFU) per millilitre.

The concentrations of microcompounds tested ranged from 15.625 µM to 500 µM. Each concentration was tested in triplicate per microcompounds per bacterial strain wells with microcompounds, alongside wells without any treatment (bacterial viability control) and well without any bacterial cell (sterility control), were alongside cultivated. The 96-well plates were incubated for 24 h at 37 °C and; after incubation, the MIC values were defined as the lowest concentration of microcompound that inhibited visible growth. The results obtained were compared to the microcompounds MIC obtained in a previous study (see the Results section) [46].

2.4 Time-kill Curves of Bacteria and SEM Imaging of *E. coli* Affected by Microcompound Treatment

Investigation bacterial growth inhibition caused by the microcompounds was performed through time-kill assays, in compliance with National Committee for Clinical Laboratory Standards protocols (NCCLS, 1999) [47]. A total of six assays were performed, two using bacteria *S. aureus* ATCC 29213 and four with *E. coli* ATCC 8739. Microcompounds were analysed at 125 µM against *S. aureus*, and at 125 µM and 62.5 µM against *E. coli*, following MICs modal values obtained. In all assays, microtubes were prepared as well as in the microdilution assays, with an initial inoculum of at 5.0×10^5 CFU·mL^{-1}.

All microtubes were incubated at 37 °C with constant stirring for 24 h. At six time points (0, 2, 5, 7, 10, and 24 h after incubation), aliquots of each sample were collected and serially diluted ten-fold in microtubes with MH (Difco®) broth. Three aliquots of 10 µL from each microtube were pipetted in MH (Difco®) agar media plates, and the plates were incubated at 37 °C for 18 h. Colonies were counted for all dilutions and treatments.

Based on time-kill differences (see Discussion), HAM pH 5δ, HAM pH 10δ, HSB L and HSB pH 10 microcompounds, alongside a positive (with $AgNO_3$) and a negative (without any treatment) control for cellular damage, were chosen as treatments for the morphological analysis by SEM of treated *E. coli* ATCC 8739. *E. coli* samples were prepared by incubation for 4 h at 37 °C in microtubes containing each a microcompound type at 125 µM, in similar conditions to the time-kill curve assay. Afterward, all microtubes were centrifuged for ten minutes at 7,000 g. Bacterial pellets were resuspended in 100 µL of deionized water, deposited in polylysine-coated (1%) glass slides, and submitted to stages of slide preparation (fixation, post-fixation, dehydration, and critical point drying) in the same manner the nanoparticles were (described in the previous section). SEM images were taken at 6,000× and 15,000× magnifications, with the latter being chosen for morphology analysis using ImageJ.

2.5 MTT Assay of Mammal Cells Treated with Centrifuged Microcompounds

The cytotoxicity of washed microcompounds was evaluated by the comparison of 3-(4,5-dimethylthiazol-2-yl)-2,5-diphenyl tetrazolium bromide (MTT-Merck®) reduction between treated and non-treated cells. The cells chosen for the assay were Macaca mulatta kidney epithelial cells (LLC-MK2 Line, CCL-7, ATCC, EUA) maintained at 5% CO_2 and 37 °C in Dulbecco's Modified

Eagle (DMEM), supplemented with 10% ($v \cdot v^{-1}$) fetal bovine serum (FBS-Invitrogen®), 2 mM of L-glutamine, 100 $IUmL^{-1}$ of penicillin, 100 $\mu g \cdot mL^{-1}$ of streptomycin and 1% ($g \cdot v^{-1}$) of tylosin. Before testing, 2×10^5 LLC-MK2 cells were cultivated in 96-well plates containing identical media, grown for 24 h, and non-adherent cells were washed away with phosphate-buffered saline solution (pH 7.2).

For the experiment, supplemented DMEM from each well was replaced with the same media now containing a type of washed microcompounds (described previously) at concentrations varying from 460 to 3680 μM (or 50 to 400 μM); and cells were cultivated for 24 h. Wells containing non-treated LLC-MK2 cells were also prepared as a positive control. Cell viability was determined by MTT (Merck®) reduction following supplier's recommendations, which were also used to determine the cytotoxicity curve and the nanoparticle concentration to inhibit cell growth by 50% (CC50).

2.6 Data Analysis

Variables in honey composition analysis are presented as mean values ± standard deviation and compared by Student's independent t-test with Welsh's correction. ImageJ measurements of SEM micrographs were compared by Mann-Whitney or Kruskal-Wallis test followed by Dunn's test; and are presented as mean values ± standard deviation. CFU numbers obtained by the time-kill curve assay are displayed and were analysed in log10. The cytotoxicity curves shown in Figures 11A and 11B were obtained through polynomial regression. All tests were performed with the statistical program GraphPad Prism version 6.02.

3. Results and Discussion

3.1 Honey Composition

Table 2 below describes the results obtained from the compositional analysis of HAM and HSB and the statistical differentiation by Student's independent t-test with Welsh's correction. In comparison to the HAM sample, HSB presented a significantly lower ($p < 0.05$) concentration of total sugars and significantly higher ($p < 0.05$) humidity, free and total acidity.

3.2 Microcompound Size Measurement by DLS

Table 3 shows the average size measurements obtained by DLS of the microcompounds synthesized using the different methods and honey samples described in this article and the ranks obtained through multiple comparison tests. Average size data is expressed in intensity, volume, number, and hydrodynamic size. The difference among the size means of a given type of microcompound attests to a polydispersity in the microcompounds. HAM microcompounds such as HAM L, HAM Lδ, HAM pH 5, and HAM pH 5δ varied in size, mostly between 350 and 620 nanometres. There is no difference between their sizes (or zeta potentials). In contrast, HAM pH 10 and HAM pH 10δ were more voluminous than the other four HAM microcompounds. Meanwhile, HAM pH 10δ presented a significantly lower average (in number) than HAM pH 10, which can be associated with the heat treatment.

Table 2. Compositional analysis of HAM and HSB samples.

Component	HAM	HSB
Ash content (%)	00.48 ± 0.01	00.59 ± 0.12
Total Reducing sugar (%)	68.94 ± 1.19	54.18 ± 2.24[1]
Humidity (%)	18.77 ± 0.92	28.13 ± 0.56[2]
Free Acidity ($mEq.kg^{-1}$)	48.66 ± 1.24	76.36 ± 0.64[2]
Lactone Acidity ($mEq.kg^{-1}$)	21.11 ± 0.32	19.29 ± 1.37
Total Acidity ($mEq.kg^{-1}$)	69.77 ± 1.43	95.65 ± 0.82[2]
Color- Brightness (L*)	21.58 ± 0.28	20.56 ± 0.23
Color: red-green scale (a*)	–1.19 ± 0.03	–0.66 ± 0.08
Color: blue-yellow scale (b*)	–4.56 ± 0.33	–5.21 ± 0.16
Whole color difference (E*ab)	2.09 (non-notable difference)	

Notes: All values (except "whole colour difference") are expressed in mean ± standard error of measurements made in triplicate. Ash content, total reducing sugars, and humidity are expressed in percentage (gg^{-1}). Free, lactone, and total acidity are expressed in milliequivalent per kilogram ($mEq.kg^{-1}$). Color and Whole color differences are noted according to the Lovibond scale. Significant differences between variables were analyzed by Welsh's t-test ($p < 0.05$). Symbols and abbreviations: HAM, Honey samples collected from *Apis mellifera* honey honeycombs; HSB, Honey samples collected from *Scaptotrigona bipunctata* honeycombs; 1, HSB average significantly lower than HAM average ($p < 0.05$); 2, HSB average significantly higher than HAM average ($p < 0.05$).

The reactions of involved in the green synthesis of silver nanoparticles (and thus microcompounds), are well described by many studies, alongside the factors involved during the process [1,2,20,48-51]. As González et al. (2016) [20] observed, glucose is the primary reducing sugar in honey, which oxidation provides electrons for nanoparticle formation, which aggregate in the silver in nanoparticles. Afterward, as Meshram et al. (2013) [51] noticed, they are then capped by molecules such as gluconic acid and proteins, forming thus the silver microcompound (or nanoparticle) and preventing further aggregation [49-51]. The

microcompounds obtained in this study varied in size and zeta potential according to the honey sample used, method of biogenic synthesis, and heating, as displayed in Table 3 and the results below.

As shown in Table 2, HAM present a greater amount of reducing sugars than HSB, thusly, HAM microcompounds presented overall smaller measurements than HSB microcompounds, in particular. Authors also have established pH to have an inverse correlation with the average size of silver particles [42-44]. Thus, the overall larger sizes of HSB microcompounds can also be related to its higher free acidity.

However, when microcompound synthesis involved basification to pH 10 (Table 3), microcompound size was greater as shown in most measurements, however HSB pH 10 and HSB pH 10δ were the smallest in number among HSB microcompounds, and smaller than their HAM counterparts. Nanoparticles tend to aggregate at highly alkaline pH values due to the high ionic strength caused by the concentration of hydroxide ions in the solution. As a result, larger structures form, which causes a difference between the average size in number and average size in intensity and volume [42-44]. Therefore, the measurements of HSB pH 10 and pH 10δ may be a result of the higher acidity of HSB.

Additionally, the heat treatment increased the average size (in number) of HAM L, HAM pH 5 and HAM pH 10 in number (Table 3); a finding that corroborates with the aggregative effect caused by increased heating time and temperature reported in the literature [42-44,52,53].

In the case of HSB microcompounds, their microcompound size reduction can be related to the fact that heat and acidity are both promoting factors for the brine electrolysis (Table 3). Furthermore, Jiang et al. (2011) [54] show that the size of nanospheres may decrease in certain conditions, such as a temperature between 32 °C and 55 °C; while additional factors, such as acidity, can favor the dissolution of particles in these conditions. The temperature range is close to the temperature of the heat treatment performed in this study. Thus the dissolution reported by Jiang et al. (2011) [54] can be related to the smaller size of HAM pH 10δ in comparison to HAM pH 10.

Therefore, the results imply the possibility that there are two events in contraposition regarding microcompound size: aggregation, favored in microcompounds synthesized with HAM and high alkalinity, and dissolution, favored by factors such as the higher free acidity of HSB. Further studies are, however, necessary to confirm this model.

Table 3. Microcompound size, obtained by Dynamic Light Scattering, in nanometers, of microcompounds produced with honey collected from *Apis mellifera* honeybees and *Scaptotrigona bipuncatata* stingless bees using different synthesis methods.

HAM Microcompounds	Size (ηm)			Hidro. size (ηm)
	Number	Intensity	Volume	
HAM L	352.27 ± 6.61	457.97 ± 12.35	600.80 ± 15.91	365,50 ± 2.69
HAM Lδ	485.80 ± 10.05	458.80 ± 10.05	601.33 ± 14.17	399,50 ± 2.55
HAM pH 5	338.43 ± 10.26	416.03 ± 8.68	531.27 ± 7.58	355,20 ± 2.96
HAM pH 5δ	487.83 ± 13.94	487.83 ± 13.94	633.30 ± 29.54	400,80 ± 0.95
HAM pH 10	1247.50 ± 136.47	2273.33 ± 241.75	3454.00 ± 84.85	1865.00 ± 119.60
HAM pH 10δ	1582.33 ± 148.54	1582.33 ± 148.54	1761.33 ± 185.21	1170.00 ± 104.80
HSB Microcompounds	Size (ηm)			Hidro. size (ηm)
	Number	Intensity	Volume	
HSB L	1035.00 ± 29.31	1195.00 ± 216.42	1102.67 ± 55.05	4916.00 ± 154.00
HSB Lδ	475.05 ± 70.36	846.00 ± 18.81	486.15 ± 76.30	7354.00 ± 130.9
HSB pH 5	740.47 ± 86.07	816.63 ± 109.29	981.57 ± 114.33	890.10 ± 29.30
HSB pH 5δ	251.07 ± 113.54	776.40 ± 99.33	989.70 ± 79.88	682.80 ± 24.86
HSB pH 10	157.40 ± 47.52	4139.50 ± 191.63	4539.50 ± 113.50	634.00 ± 7.30
HSB pH 10δ	442.93 ± 99.45	1090.00 ± 113.71	1170.33 ± 42.50	683.00 ± 4.13

Notes: Size measurements are displayed in mean ± standard deviation. Abbreviations: HAM, Microcompounds with honey samples collected from *Apis mellifera* honey honeycombs; HSB, Microcompounds with honey samples collected from *Scaptotrigona bipunctata* honeycombs; Hidro. Size, Hydrodynamic size; L, microcompound obtained by light exposure; Lδ, microcompound obtained by light exposure and heating; pH 10, microcompound obtained by "aggregating basification"; pH 10δ, microcompound obtained by "aggregating basification" and heating; pH 5; microcompound obtained by "basification"; pH 5δ, microcompound obtained by "basification" and heating.

Another possible effect of using a honey sample with a higher concentration of free acidity (such as HSB) for microcompound synthesis is the alteration of its surface charge. Table 4 displays and compares the zeta potential of microcompounds produced with HAM and HSB.

Table 4. Zeta potential of microcompounds produced with honey collected from *Apis mellifera* honeybees (HAM) and honey collected from *Scaptotrigona bipunctata* stingless bees (HSB) obtained by electrophoretic mobility inspection of surface charges.

HAM Microcompound	Zeta potential (mV)	HSB Microcompound	Zeta potential (mV)
HAM L	–0.436 ± 0.06	HSB L	+2.31 ± 0.21
HAM Lδ	–0.469 ± 0.03	HSB Lδ	+0.941 ± 0.063
HAM pH 5	–0.628 ± 0.09	HSB pH 5	+0.283 ± 0.045
HAM pH 5δ	–0.703 ± 0.03	HSB pH 5δ	+1.91 ± 0.46
HAM pH 10	–5.28 ± 0.21	HSB pH 10	–4.22 ± 0.415
HAM pH 10δ	–3.8 ± 0.51	HSB pH 10δ	–9.07 ± 1.1

Notes: Size measurements are displayed as mean ± standard deviation. Symbols and abbreviations: HAM, Microcompounds with honey samples collected from Apis mellifera honey honeycombs; HSB, Microcompounds with honey samples collected from Scaptotrigona bipunctata honeycombs; L, microcompound obtained by light exposure; Lδ, microcompound obtained by light exposure and heating; pH 10, microcompound obtained by "aggregating basification"; pH 10δ, microcompound obtained by "aggregating basification" and heating; pH 5; microcompound obtained by "basification"; pH 5δ, microcompound obtained by "basification" and heating.

In regards to zeta potential, zeta potentials of HSB microcompounds presented greater modular charges than the corresponding HAM microcompound in four out of six cases. In other words, only in cases which microcompounds were obtained by basification without heat treatment HAM microcompounds obtained a greater charge. Our data also show that HSB microcompounds (HSB L, HSB Lδ, HSB pH 5, HSB pH 5δ) have a positive surface charge, except in microcompounds with high alkalinity (HSB pH 10 and HSB pH 10δ). The results also indicate that high alkaline synthesis processes can grant a negative charge and increase it (as well as provide a high ionic force), as seen with HAM pH 10, HAM pH 10δ, HSB pH 10, and HSB pH 10δ (Table 4). This characteristic has many pharmacological implications: for example, the pH of many tissues targeted by pathogenic bacteria is acidic; consequently, microcompounds with a positive surface charge can present higher stability in those environments [55-57]. Additionally, given that the cell wall of most bacteria is negatively charged, microcompounds with a positive charge potential have a greater tendency to bind to the structure. Authors such as Radovic-Moreno et al. (2012) [56] and Qiao et al. (2018) [58] have developed effective surface-changing antibacterial delivery systems, and Abbaszadegan et al. (2014) [59] noted that nanoparticles with positive charge have a better antibacterial effect against Gram-positive and Gram-negative bacteria.

3.3 SEM Images and Measurements of Centrifuged Particles inside Microcompounds

The micrographs in Figure 2, taken at 20000× by SEM, show the round morphology and size of silver particles inside each microcompound, while size averages (as equivalent circular diameter- ECD), roundness, and circularity values are presented in Table 5, alongside significant differences demonstrated by Dunn's and Kruskal-Wallis tests.

The average size (ECD) among the silver particles inside all types of microcompounds varied between 100 nm and 150 nm; and thus, can be considered a mixture of nanoparticles and fine particles [60-63]. Significant differences ($p < 0.05$) found in particle size averages were not corelated to microcompound average sizes measured by DLS. For example, while HSB usage resulted in microcompounds significantly larger overall, the average particle diameter of HSB microcompounds do not have significant differences in four cases. They are significantly smaller ($p < 0.05$) in the other two groups: in the "L" and "pH 5" groups (without heat treatment).

HAM pH 10 and HAM pH 10δ microcompounds had larger agglomerates (Table 2); however, the particles inside the "larger" HAM pH 10 and HAM pH 10δ microcompounds were significantly smaller ($p < 0.05$) than those in HAM L, HAM Lδ, HAM pH 5 and HAM pH 5δ (Table 5). This finding can be related to the inverse correlation between pH and particle size, previously discussed [42-44]. Furthermore, the paired comparison of particle sizes between heated and non-heated microcompounds showed that the heat treatments significantly reduced ($p < 0.05$) the average size of particles inside HAM Lδ and HAM pH 5δ in comparison to HAM L and HAM pH 5.

As for the particles' morphology, the silver nanoparticles were revealed to be somewhat elongated, presenting circularity averages between 0.20 and 0.35, and generally round, presenting roundness averages between 0.64 and 0.74 among all types. These results (shown in Table 5 and Figure 2) show that the effect of a given variable (honey choice, synthesis method…) can vary depending on the other factor involved. For example, even though silver particles in HSB pH 10 presented an even significant-

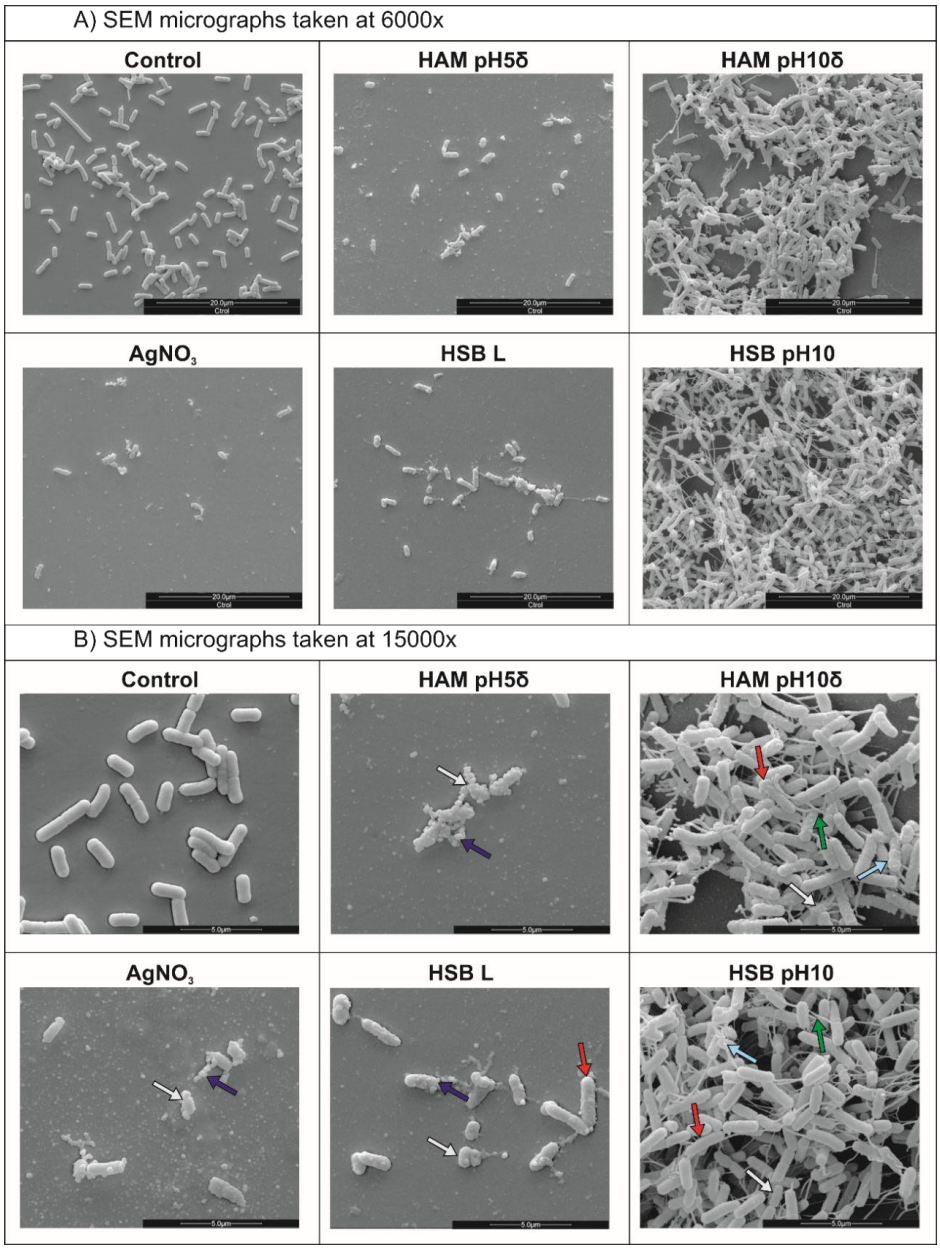

Figure 2. Selected Scanning Electron Microscopy images of silver particles inside each type of microcompound.

Notes: All images were taken at 20000× magnification, and Dunn's multiple comparison test compared variables (size, roundness, and circularity). They are ordered from A to L, based on the microcompound type in the image as follows: (A) HAM L, (B) HAM Lδ; (C) HAM pH 5, (D) HAM pH 5δ, (E) HAM pH 10, (F) HAM pH 10δ, (G) HSB L, (H) HSB Lδ, (I) HSB pH 5, (J) HSB pH 5δ, (K) HSB pH 10, (L) HSB pH 10δ. The red circles show silver particles inside the HSB L and HSB Lδ microcompounds, with the latter portraying higher ratios of roundness and circularity after undergoing the described heat treatment. Blue circles display images of HAM pH 5δ and HAM pH 10δ particles, which exemplify how the higher degree of basification may result in smaller and more elongated particles. Lastly, the yellow circles point to HAB MB and HSB pH 5 particles, demonstrate how using HSB honey in the same synthesis method resulted in particles with smaller average size, roundness, and circularity ratios. Symbols and abbreviations: HAM, Honey samples collected from *Apis mellifera* honey honeycombs; HSB, Honey samples collected from *Scaptotrigona bipunctata* honeycombs; L, microcompound obtained by light exposure; Lδ, microcompound obtained by light exposure and heating; pH 10, microcompound obtained by "aggregating basification"; pH 10δ, microcompound obtained by "aggregating basification" and heating; pH 5; microcompound obtained by "basification"; pH 5δ, microcompound obtained by "basification" and heating.

Table 5. Average size, roundness and circularity ratios of silver particles inside the microcompounds captured Scanning Electron Microscopy micrographs.

HAM Micro.	Calculated diameter (nm)	Roundness	Circularity
HAM L	$134.7 \pm 83.05^{a,>,\oplus}$	$0.7412 \pm 0.16^{a,>,\oplus}$	$0.3112 \pm 0.15^{a,>,\oplus}$
HAM Lδ	115.4 ± 64.28^{a}	$0.6889 \pm 0.14^{a,\oplus}$	$0.2009 \pm 0.44^{c,\otimes}$
HAM pH 5	$149.3 \pm 114.5^{a,\oplus}$	0.6671 ± 0.14^{b}	$0.2850 \pm 0.14^{ab,<,\oplus}$
HAM pH 5δ	121 ± 65.42^{a}	0.6508 ± 0.18^{b}	$0.3536 \pm 0.18^{a,\oplus}$
HAM pH 10	$112 \pm 62.9^{b,>}$	$0.7126 \pm 0.15^{ab,>}$	0.2717 ± 0.12^{b}
HAM pH 10δ	93.38 ± 54.62^{b}	$0.6629 \pm 0.17^{ab,\otimes}$	$0.2579 \pm 0.11^{b,\otimes}$
HSB Micro.	Calculated diameter (nm)	Roundness	Circularity
HSB L	93.38 ± 54.62^{a}	$0.6819 \pm 0.16^{b,>}$	$0.2309 \pm 0.10^{b,<}$
HSB Lδ	114.20 ± 64.75^{a}	0.6382 ± 0.22^{b}	0.2785 ± 0.15^{b}
HSB pH 5	128.1 ± 57.72^{a}	0.6739 ± 0.16^{b}	0.2163 ± 0.10^{b}
HSB pH 5δ	105.9 ± 70.16^{b}	0.6906 ± 0.17^{a}	0.2470 ± 0.14^{b}
HSB pH 10	108.0 ± 51.25^{a}	0.7399 ± 0.15^{a}	$0.2709 \pm 0.12^{a,<}$
HSB pH 10δ	118.5 ± 68.06^{b}	0.7101 ± 0.16^{a}	0.3569 ± 0.17^{a}

Notes: Values are displayed as mean ± standard deviation. The diameter was calculated through the formula: $A = \pi(\text{diameter}/2)^2$. Ranks were detected by Dunn's multiple comparisons of HAM (or HSB) microcompounds and shown through letters. The "a" rank was attributed to the highest mean, and the other ranks were given letters based on significant difference, and means that share one letter are not significantly different. Symbols indicate significant differences ($p < 0.05$) detected by the Kruskal-Wallis test. Symbols and abbreviations: $\oplus$, Significantly greater value ($p < 0.05$) than corresponding HSB; $\otimes$, Significantly lower value ($p < 0.05$) than corresponding HSB microcompound; >, Significantly greater value ($p < 0.05$) than corresponding heated microcompound; <, Significantly lower value ($p < 0.05$) than corresponding heated microcompound; HAM, Microcompounds with honey samples collected from *Apis mellifera* honey honeycombs; HSB, Microcompounds with honey samples collected from *Scaptotrigona bipunctata* honeycombs; L, microcompound obtained by light exposure; Lδ, microcompound obtained by light exposure and heating; Micro., microcompound; pH 10, microcompound obtained by "aggregating basification"; pH 10δ, microcompound obtained by "aggregating basification" and heating; pH 5; microcompound obtained by "basification"; pH 5δ, microcompound obtained by "basification" and heating.

ly higher roundness ratio than the corresponding HAM pH 10, particles inside HAM L were overall rounder than those in HSB L (Table 5). Therefore, honey-mediated synthesis of microcompounds containing silver nanoparticles can be optimized the choices of honey sample, synthesis method, and post-synthesis treatments like heating.

HAM L and HSB pH 10 showed the highest roundness values among the HAM and HSB groups, respectively, while particles inside HAM pH 5δ and HSB Lδ the presented the lowest ones. HAM L particles had significantly higher roundness ratios ($p < 0.05$) than HAM pH 5's, and HAM pH 10 particles do not have a significantly different roundness ($p < 0.05$) than either. Meanwhile, among the particles in HSB microcompounds, HSB pH 5δ, HSB pH 10 and HSB pH 10δ were significantly lower ($p < 0.05$) than all others in HSB. In relation to the "honey sample" used, HAM L and HAM Lδ presented significantly ($p < 0.05$) higher "roundness" than HSB L and HSB Lδ, respectively. As for the circularity of particles, heating seems to result in more circular HSB nanoparticles (Table 5).

3.4 MIC Assays of before and after Centrifugation

Table 6 displays Minimal Inhibitory Concentrations (MICs)- estimated by Ag concentration obtained through atomic absorption spectroscopy - of washed HAM and HSB microcompounds, against *S. aureus* ATCC 29231 and *E. coli* ATCC 8739, and compared against microcompound MICs (without centrifugation) described in a previous article [46].

MIC of all non-centrifuged microcompounds in a previous analysis [46] varied between 15 µM and 250 µM (or 1.62-27 $\mu g \cdot mL^{-1}$) and were similar to MIC findings described in the literature, and thus a promising result [67-77]. However, MIC against *E. coli* and *S. aureus* strains increased for most types of microcompounds centrifuged from the honey solution (Table 6). This noticed increase alludes to the relevance of the honey present in the solution as an antibacterial factor, as described by literature [35-40]. HSB pH 10 and HSB pH 10δ MIC lowered after microcompound washing, which might be related to two compounded factors. HSB's main antibacterial effect (the oxygen peroxide

Table 6. Minimal Inhibitory Concentrations (MICs) of silver particles obtained with honey collected from *Apis mellifera* honeybees.

HAM Micro.	*Escherichia coli* ATCC 8739 MIC (μM)		*Staphylococcus aureus* ATCC 29231 MIC (μM)	
	Micro.	Washed micro.	Micro.	Washed micro.
HAM L	62.5	125 (2)	62.5	62.5 (1)
HAM Lδ	62.5	250 (4)	62.5	125 (2)
HAM pH 5	125	250 (2)	250	500 (2)
HAM pH 5δ	125	125 (1)	250	500 (2)
HAM pH 10	62.5	125 (2)	31.25	250 (8)
HAM pH 10δ	62.5	250 (4)	31.25	125 (4)
$AgNO_3$	62.5	62.5	62.5	62.5
HSB Micro.	*Escherichia coli* ATCC 8739 MIC (μM)		*Staphylococcus aureus* ATCC 29231 MIC (μM)	
	Micro.	Washed micro.	Micro.	Washed micro.
HSB L	62.5	125 (2)	62.5	125 (2)
HSB Lδ	62.5	125 (2)	62.5	125 (2)
HSB pH 5	62.5	250 (4)	250	250 (1)
HSB pH 5δ	62.5	125 (2)	250	500 (2)
HSB pH 10	62.5	31.25 (0.5)	125	62.5 (0.5)
HSB pH 10δ	62.5	62.5 (1)	125	62.5 (0.5)
$AgNO_3$	62.5	62.5	62.5	62.5

Notes: The Microcompound MIC values were shown in a previous article [45]. Washed microcompounds were obtained by centrifugation. Symbols and abbreviations: $AgNO_3$, Silver nitrate; ATCC, American Type Culture Collection; Washed microcompounds, microcompound obtained through centrifugation; HAM, Microcompounds with honey samples collected from *Apis mellifera* honey honeycombs; HSB, Microcompounds with honey samples collected from *Scaptotrigona bipunctata* honeycombs; L, microcompound obtained by light exposure; Lδ, microcompound obtained by light exposure and heating; MIC, Minimal Inhibitory Concentration (μM); Micro, Microcompound, pH 10, microcompound obtained by "aggregating basification"; pH 10δ, microcompound obtained by "aggregating basification" and heating; pH 5; microcompound obtained by "basification"; pH 5δ, microcompound obtained by "basification" and heating.

production by glucose oxidase) is reported by Brudzynski (2020) [78] to be compromised by high alkalinity; and the partial removal of stabilizing agents, such as gluconic acid, promoted an increase in the silver release [36,38,51,78]. Further studies are necessary in order to confirm this theory.

3.5 Time-kill Curve of Bacteria Exposed to Microcompounds

Figures 3A-3F display the effects of HAM and HSB microcompounds on the bacterial growth of *E. coli* ATCC 8739 and *S. aureus* ATCC 29213 and of $AgNO_3$ treatment. Effects are analyzed based on CFU counts after hours of microcompound treatments, and the graphs show the data as logarithms with base 10 of the number of colonies forming units per milliliter (log10 $CFU \cdot mL^{-1}$). Supplementary Tables 1A through 1F compare the antibacterial potential of microcompounds by displaying the multiple comparison rankings based on microcompound treatment and time stamp; while supplementary Tables 2A, 2B, and 2C, meanwhile, show the comparison of the CFU reduction (compared to the positive control) between each HAM microcompound and its corresponding HSB counterpart.

In general, the Gram-negative strain (*E. coli* ATCC 8739) demonstrated higher sensitivity than the Gram-positive, as observed in the significantly greater ($p < 0.05$) log10 reduction in assays involving *E. coli* (Figures 3E and 3F and suppl. Tables 1E and 1F). Against *S. aureus* ATCC 29231, HAM microcompounds presented a significantly lower log10 CFU than control ($p < 0.05$) only after 4 h (Figure 3A, suppl. Table 1A). HSB microcompounds, in contrast, presented a lower log10 CFU than control after two hours in all cases ($p < 0.05$; Figure 3B, suppl. Table 1B) and thus a greater log reduction than HAM microcompounds (suppl. Table 2A). Even after halving treatment concentration for time-kill assays with *E. coli*, the Gram-negative strain still presented lower CFU counts at the last timestamps (10 h and 24 h).

The greater sensitivity of Gram negative bacterial to nanoparticles is well established in current literature,

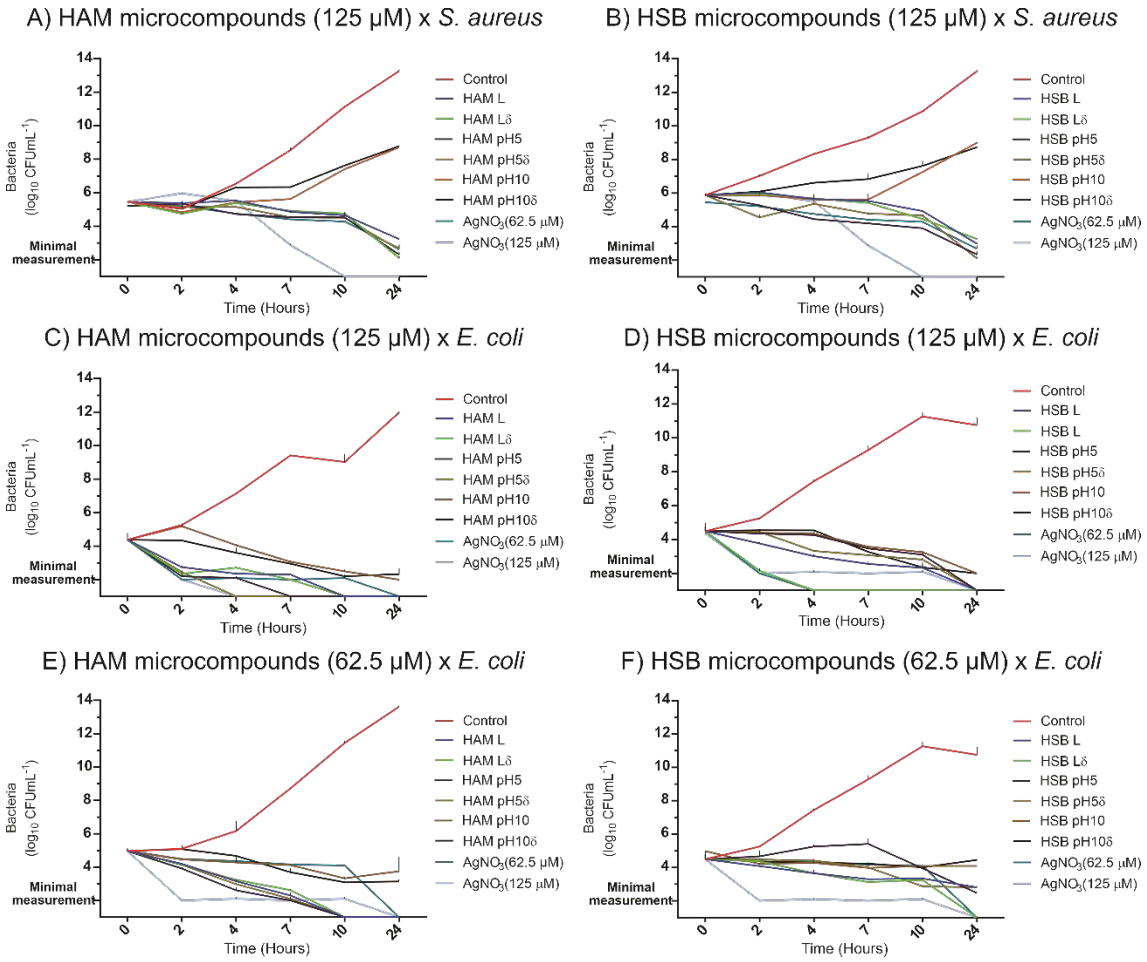

Figure 3. Time-kill curves *Staphylococcus aureus* and *Escherichia coli* exposed to microcompounds and multiple comparison of CFU counts.

Notes: Time-kill curves are displayed as mean ± standard deviation in Figure 3, and ranks attributed by Dunn's multiple comparison test in the supplementary material. Bacterial growth without exposure to any treatment is denominated control; and the minimal value of 1.0×10^2 was adopted due to methodological limitations. Graphs in Figure 3 are divided as follows: (A) Time-kill curves of *Staphylococcus aureus* ATCC 29231 exposed to HAM microcompounds at 125 µM. (B) Time-kill curves of *Staphylococcus aureus* ATCC 29231 exposed to HSB microcompounds at 125 µM. (C) Time-kill curves of *Escherichia coli* ATCC 8739 exposed to HAM microcompounds at 125 µM. (D) Time-kill curves of *Escherichia coli* ATCC 8739 exposed to HSB microcompounds at 125 µM. (E) Time-kill curves of *Escherichia coli* ATCC 8739 exposed to HAM microcompounds at 62.5 µM. (F) Time-kill curves of *Escherichia coli* ATCC 8739 exposed to HSB microcompounds at 62.5 µM. Statistical analysis of CFU data is displayed in the "Supplementary Data" section. Abbreviations: $AgNO_3$, Silver nitrate solution in different concentrations; HAM, Honey samples collected from *Apis mellifera* honey honeycombs; HSB, Honey samples collected from *Scaptotrigona bipunctata* honeycombs; L, microcompound obtained by light exposure; Lδ, microcompound obtained by light exposure and heating; pH 10, microcompound obtained by "aggregating basification"; pH 10δ, microcompound obtained by "aggregating basification" and heating; pH 5; microcompound obtained by "basification"; pH 5δ, microcompound obtained by "basification" and heating.

which notes that the greater stiffness and extension wall of Gram-positive bacteria grant partial protection [69,77,79,80]. However the reducing and stabilizing agent, honey, has a greater effect against Gram-positive strains [12,36,38,80-82]. Thus, the microcompounds described in this article show the potential to have a broader spectrum of activity due to the choice of stabilizing agent for the silver nanoparticles (honey).

Against *E. coli*, microcompounds such as HAM Lδ and HSB pH 5, achieved a bactericidal effect similar to silver nitrate ($AgNO_3$)- as observed in Figures 3C-3F and suppl. Tables 1C-1F. The antibacterial efficiency of HSB Lδ and HAM pH 5δ 100% of of *E. coli* after application of some microcompounds (HSB Lδ and HAM pH 5δ)

after 4 h at 125 μM (Figures 3C and 3D; suppl. Tables 1C and 1D) warranted another analysis at 62.5 μM (Figures 3E and 3F; suppl. Tables 1E and 1F). Even then, microcompounds synthesized through light exposure (HAM L, HAM Lδ, HSB L, HSB Lδ) or regular basification (HAM pH 5, HAM pH 5δ, HSB pH 5, HSB pH 5δ) presented a bactericidal effect.

HAM pH 10, HAM pH 10δ, HSB pH 10, and HSB pH 10δ, however, obtained by aggregating basification, did not perform well as the other microcompounds. They were only effective in containing the *S. aureus* and *E. coli* growth at 125 μM after 24 h, showing a significantly higher CFU at 24 h compared to the beginning of the assay. This difference can be related to both the high ionic force and surface charge presented by those microcompounds (Tables 2 and 3), given that the negative charge hampers electrostatic attraction to bacterial cells and the agglomeration of silver particles in highly alkaline environments goes against the release of silver ions (and thus the antibacterial effect of the particle) [9,14,59].

As for the comparison in CFU count between honey samples, while HAM and HSB microcompounds presented antibacterial properties against *E. coli* and *S. aureus*, HSB microcompounds exhibited a more pronounced antibacterial effect against the *S. aureus*; while HAM microcompounds caused a more significant reduction in *E. coli* (Figure 3). This finding might be related to the antibacterial property HSB itself has, as data obtained from a previous study indicate this honey sample to be particularly effective against *S. aureus* [36].

Other differences between HAM and HSB microcompounds might also stem from differences in the antibacterial effect of the particles themselves, as HAM microcompounds present a more intense bactericidal effect even in a concentration much lower than the established MIC for HAM [36]. Those findings further suggest the potential for exploration in studies of honey-microcompound interactions, given Rani, Rao, Shamili & Padmaja (2018) [83] have already described a silver-honey combination helpful in wound healing.

No microcompound was the best in all cases, nor was a "factor" in the microcompound production (honey sample used, synthesis method, or heat treatment) that improved the antibacterial effect in all cases. Among all HAM microcompounds, HAM pH 5δ and HAM pH 5 inhibited *E. coli* growth the fastest (Figure 3C); and, among HSB microcompounds, the HSB L was particularly effective against the Gram-negative strain (Figure 3D). However, against *S. aureus*, HAM Lδ and HSB pH 5δ presented the lowest log10 CFU counts among HAM and HSB microcompounds, respectively, after 24 h (Figures 3A and 3B).

Lastly, the antibacterial efficiency of HAM and HSB microcompounds is comparable to the antibacterial effect of other silver nanoparticles described in literature. Table 7 compares the concentration of silver nanoparticles in microcompounds which reached 100% antibacterial efficiency in our work with concentrations of other silver nanoparticle described in literature. Compared to current literature about the antibacterial effect, of silver nitrate and silver nanoparticles synthetized through other methods, silver nitrate had a slower effect (at a similar concentration), while our microcompounds with silver nanoparticles demonstrated were bactericidal at low concentrations, while they required more time for their antibacterial effect.

In summary, the results reveal that the differences between the antibacterial effects of microcompounds depend on the honey sample used, method of microcompound synthesis, and bacterial model, and that certain combinations, might result in microcompounds with antibacterial effects of particular potential. While this implies the necessity of more studies to assert conclusions, they also show how perspective the analysis of factors involved in the biogenic synthesis of silver microcompounds can be.

3.6 SEM Images and Measurements of *E. coli* Affected by Microcompound Treatments

Figure 4 contains SEM images captured at 6000× and 15000× of *E. coli* ATCC 8739 submitted to microcompound treatments for 4 h (compared to control). It also pinpoints morphological alterations through arrows in figure. Additionally, results concerning the average bacterial cell size, circularity, and roundness ratios were measured using ImageJ Photoshop, statistically analyzed by Dunn's multiple comparison test, and are exhibited in Table 8.

The white arrows in Figure 4A showed treated *E. coli* cells smaller than control, and this difference is confirmed to be statistically significant ($p < 0.05$) in the analysis of measurements taken (Table 8). The application of microcompound treatments also resulted in blebbing as well (light and dark blue arrows, correspondingly); however, its severity varied between treatment was applied, given the significantly lower circularity ratio ($p < 0.05$) of HAM pH 5δ and $AgNO_3$ cells. Cell filamentation and cell biofilm formation were observed (red and green arrows), with the latter being present particularly in *E. coli* treated with HAM pH 10δ and HSB pH 10. There was no significant difference ($p > 0.05$) in the roundness ratio of the measured cells (Figure 4).

The SEM micrographs in figures 4A and 4B exhibited several morphological alterations of *E. coli* cells esteeming from the application of microcompounds at 125 μM,

Table 7. Minimal Bactericidal Concentrations (MBCs) of silver coumpounds obtained through different methods described in literature.

Type of silver compound	Tested bacterial strain(s)	Concentration (in μM)	Time for 100% efficacy	Reference
Silver nanoparticles in microcompouds with honey	*S. aureus* ATCC 29231 *E. coli* ATCC 29231	125 125 62.5	24 hours* 4 hours 24 hours	Our findings
Silver nitrate	*E. coli* O104:H14 *E. coli* O157:H7 *P. aeruginosa* (not specified) MRSA (not specified)	55.63	1 hour	Mohamed et al. (2012) [84]
AgNP synthetized with *Camellia sinensis* leaf extract	*E. coli* ATCC 25922 *K. pneumoniae* ATCC 13773 *S.* Typhimurium ATCC 14028 *S.* Enteritidis ATCC 13076	290 144.6 72.3 72.3	2 hours 1 hour 2 hours 2 hours	Loo et al. (2018) [85]
AgNP synthetized with *Ocimum gratissimum* leaf extract	Multidrug resistant *E. coli* (MC-2) Multidrug resistant *S. aureus* (MMC-20)	74.7 149.5	8 hours	Das et al. (2015) [86]
AgNP synthetized with *Ocimum gratissimum* ethanol extract	*S.* Enteritidis (CMPZCSB1)	58	7 hours*	Abdelsattar et al. (2022) [87]
AgNP synthetized with *Ocimum gratissimum* ethanol extract	*S.* Enteritidis (CMPZCSB1)	58	7 hours*	Abdelsattar et al. (2022) [87]
AgNP synthetized through basification	*H. pylori* NCTC 11673	37.1	24 hours	Amin et al. (2014) [88]

Notes: Silver nanoparticle concentrations described in literature were converted in micromolar (μM). In cases which 100% efficacy was not observable, the time for >99.9% efficacy was listed. Abbreviations: AgNP, silver nanoparticles; *E. coli*, *Escherichia coli*; *H. pylori*, *Heliobacter pylori*; *K. pneumoniae*, *Klebesiella pneumoniae*; MRSA, methicillin-resistant *Staphylococcus aureus*; *P. aeruginosa*, *Pseudomonas aeruginosa*; *S. areus*, *Staphylococcus aureus*; *S.* Enteretidis, S*almonella enterica* serovar Enteretidis; S. Typhimurium, *Salmonella enterica* serovar Thyphimurium.

which varied depending on the microcompound type used. It is noticeable that cell density is lower in the treated samples images than the control one, and the micrographs of antibacterial micromcompounds treatments ($AgNO_3$, HAM pH 5δ, and HSB L) presented fewer bacterial cells than the bacteriostatic ones (HAM pH 10δ and HSB pH 10). Notably, after those treatments, bacterial cells presented severe blebbing (Figure 4, dark blue arrows) centered in the poles, similar to silver's effect in $AgNO_3$ and the oxidative stress caused by honey treatments [36,89-91]. The average size of bacteria-treated microcompound cells was significantly lower ($p < 0.05$) than control (Figure 4, white arrows and Table 8). This effect of microcompounds has been observed in bacteria treated with peptidoglycan (ampicillin) and protein (erythromycin) synthesis inhibitors [89].

Additionally, the elongation of treated *E. coli* cells observed in cells treated with HSB L, HAM pH 10δ, and HSB pH 10 (Figure 4, red arrows), denominated "filamentation" in *E. coli*, is attributed to the inhibition of enzymes critical in septation (such as penicillin-binding protein 3) and to responses to DNA damage, mediated by the SOS pathway or not [89,92-95]. In conjunction with other authors, Lee, Kim and Lee (2014) [96] repost that silver nanoparticles can cause *E. coli* elongation by ROS-related DNA damage, which triggers an SOS response in the bacteria [96-99]. This corroborates our findings, as the use of HAM pH 10δ and HSB HAM treatments are not bactericidal at 125 μM (Figures 3C and 3D) and thus allow in turn *E. coli* to respond to their effects, which results in filamentation (Figure 4).

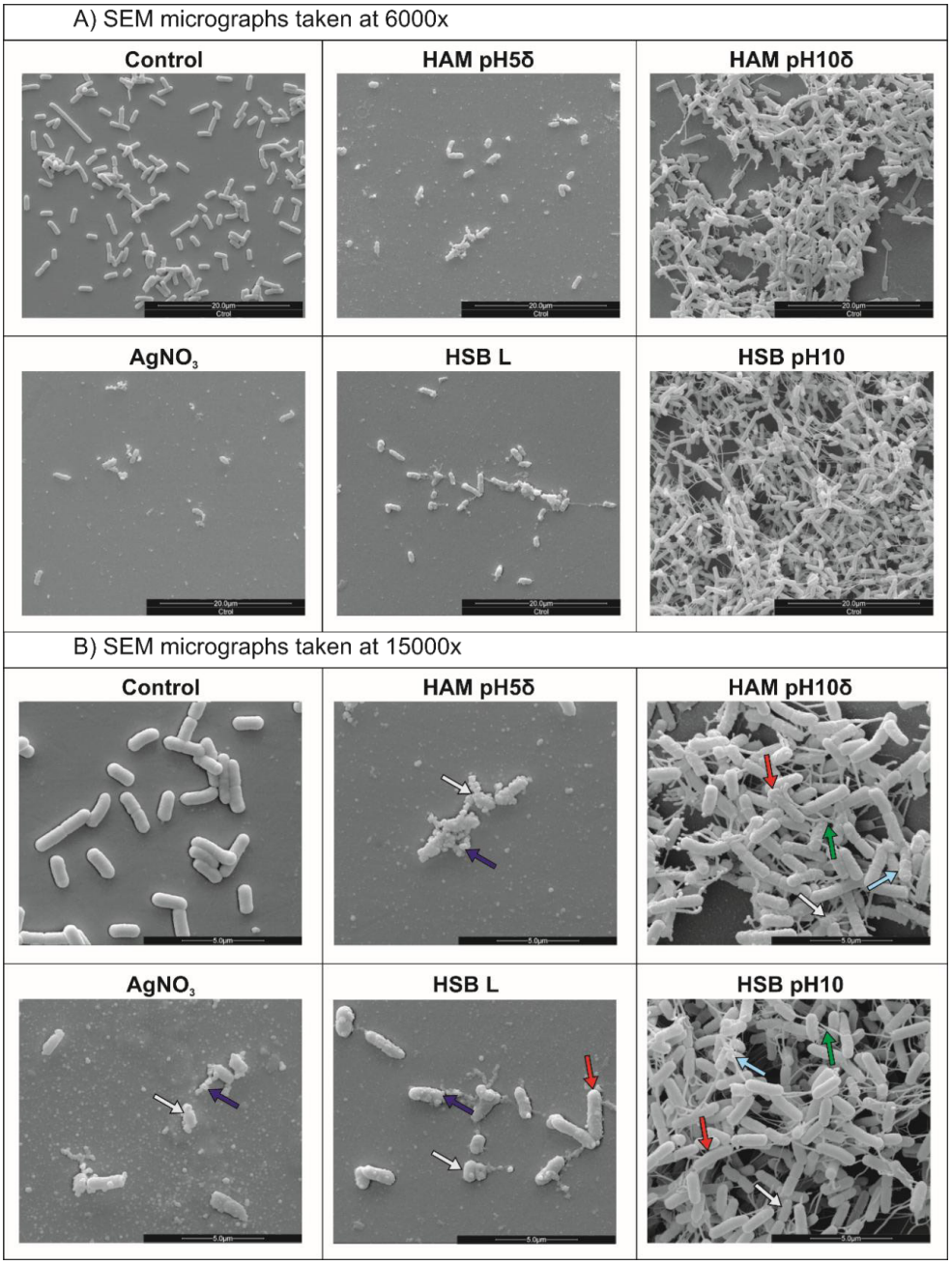

Figure 4. Scanning Electron Microscopy images of *Escherichia coli* ATCC 8739 cells after microcompound treatment.

Notes: Micrographs in Figure 4A and 4B were taken at 6000× and 15000×, respectively

Notes: Bacterial cells are named after the microcompounds treatment they were submitted to during the 4h of incubation. White arrows in image 8B show examples of bacterial cells smaller than those submitted to control conditions. The following morphological alterations were noted among different treatments: Severe and light blebbing (dark and light blue arrows); cell filamentation- i.e., abnormal growth- (red arrows); and biofilm formation (green arrows). Symbols and abbreviations: $AgNO_3$, Silver nitrate; HAM, Microcompounds with honey samples collected from *Apis mellifera* honey honeycombs; HSB, Microcompounds with honey samples collected from *Scaptotrigona bipunctata* honeycombs; L, microcompound obtained by light exposure; Lδ, microcompound obtained by light exposure and heating; pH 10, microcompound obtained by "aggregating basification"; pH 10δ, microcompound obtained by "aggregating basification" and heating; pH 5; microcompound obtained by "basification"; pH 5δ, microcompound obtained by "basification" and heating.

Table 8. Average size, roundness and circularity ratios of *Escherichia coli* ATCC 8739 cells affected by microcompound treatments captured Scanning Electron Microscopy images (compared to control).

Microcompound treatment	Area (μm^2)	Roundness	Circularity
Control	3.012 ± 0.54^a	0.706 ± 0.05^a	0.4534 ± 0.07
$AgNO_3$	1.527 ± 0.55^b	0.4989 ± 0.13^b	0.5191 ± 0.18
HAM pH 5δ	1.353 ± 0.57^b	0.638 ± 0.11^{ab}	0.4939 ± 0.10
HSB L	1.337 ± 0.44^b	0.6085 ± 0.10^{ab}	0.395 ± 0.12
HAM pH 10δ	1.611 ± 0.66^b	0.5739 ± 0.98^{ab}	0.3238 ± 0.08

Notes: Values are displayed as mean ± standard deviation. Differences were detected by Dunn's multiple comparisons between microcompounds and shown through symbols ($p < 0.05$). The "a" rank was attributed to the highest mean, and the other ranks were given letters based on significant difference, and means that share one letter are not significantly different ($p > 0.05$). Symbols and abbreviations: $AgNO_3$; silver nitrate; HAM, Microcompounds with honey samples collected from *Apis mellifera* honey honeycombs; HSB, Microcompounds with honey samples collected from *Scaptotrigona bipunctata* honeycombs; L, microcompound obtained by light exposure; Lδ, microcompound obtained by light exposure and heating; pH 10, microcompound obtained by "aggregating basification"; pH 10δ, microcompound obtained by "aggregating basification" and heating; pH 5; microcompound obtained by "basification"; pH 5δ, microcompound obtained by "basification" and heating.

The honey samples present in the microcompoumds might also contribute to this effect; Brudzynski and Sjaarda (2014) [100] attribute it to Canadian honey samples, while this morphological alteration is not present among the bacteria treated with $AgNO_3$ or HAM pH 5δ due to how their metabolism comprise by the treatments applied. Lastly, elongation has also been related to an abnormal cell division caused by novobiocin [82,89,101-103]. Thus, from our results in conjunction with established literature, it can be deduced that all microcompound treatments used can compromise bacterial multiplication by different mechanisms.

SEM images also showed biofilm production after HAM pH 10δ or HSB pH 10 treatments (Figure 4, green arrows). Though nanoparticles treatments present antibiofilm properties, this shows that conditions in microcompound synthesis can negatively affect this antibacterial mechanism [104]. Therefore, SEM imagining can be used to verify the presence of resistant mechanisms against silver microcompounds and to observe similarities between the effect of microcompounds and silver nanoparticles.

Figure 5 summarizes the morphological alterations observed in *E. coli* treated with microcompounds and the proposed mechanisms involved based on literature.

3.7 Cytotoxicity of Cells Treated with Silver Nanoparticles

The polynomial regression curves in Figure 6 show the viability rates of LLC-MK2 cells treated with HAM and HSB silver microcompounds (compared to control), while Table 9 exhibits the CC50 and selectivity indexes of microcompound treatments. Honey excess was removed before the assays, as can interfere in MTT readings and present in vitro cytotoxicity at higher concentrations (even is though it is safely consumed) [105,106].

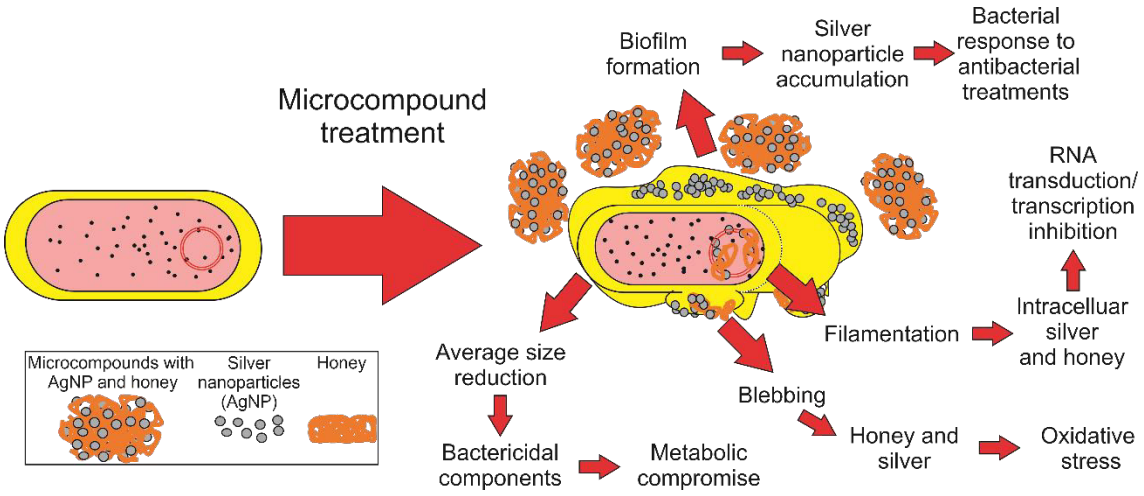

Figure 5. Morphological alteration observed in *E. coli* ATCC 8739 treated with HAM and HSB microcompounds and the proposed mechanisms involved.

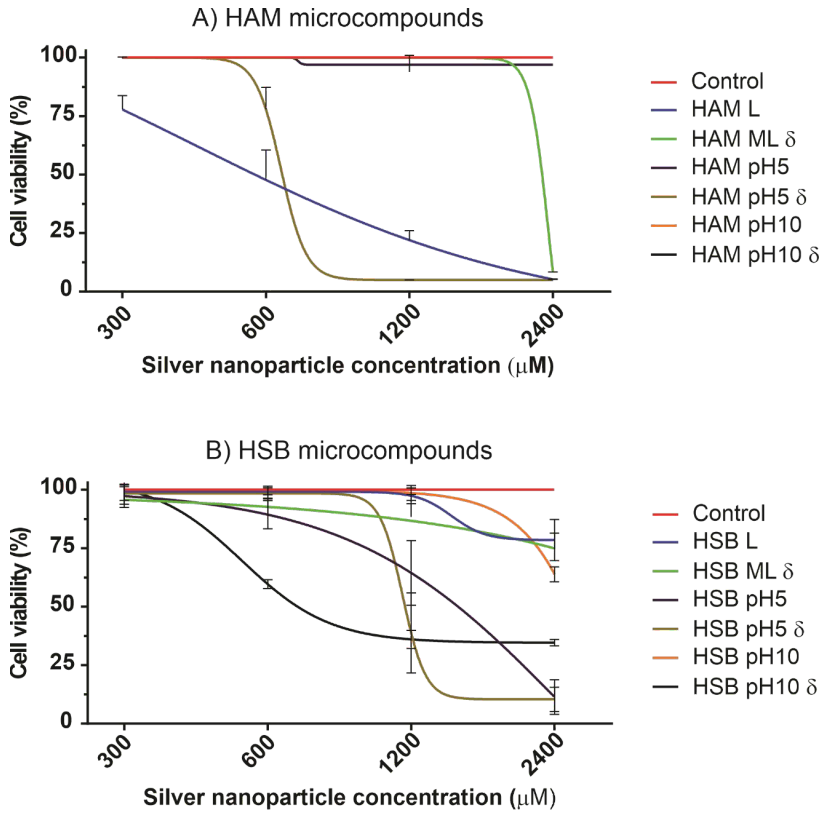

Figure 6. LLC-MK2 viability curves obtained by polynomial regression after treatments with HAM and HSB microcompounds.

Notes: LLC-MK2 viability curves were obtained by polynomial regression of MTT assays of cells after (A) HAM and (B) HSB microcompound treatments at chosen concentrations. Symbols and abbreviations: Control, LLC-MK2 not submitted to any nanoparticle treatment; HAM, Microcompounds with honey samples collected from *Apis mellifera* honey honeycombs; HSB, Microcompounds with honey samples collected from *Scaptotrigona bipunctata* honeycombs; L, microcompound obtained by light exposure; Lδ, microcompound obtained by light exposure and heating; LLC-MK2; Cell line of *Macaca mulatta* kidney epithelial cells; pH 10, microcompound obtained by "aggregating basification"; pH 10δ, microcompound obtained by "aggregating basification" and heating; pH 5; microcompound obtained by "basification"; pH 5δ, microcompound obtained by "basification" and heating.

The microcompound treatments did not compromise LLC-MK2 viability at the concentration 300 μM, higher than the antibacterial concentrations analyzed earlier. Only HAM L showed significantly lower cell viability at that concentration ($p < 0.05$), and mammal cells were still viable even after applications of HSB L, HSB L, HSB pH 10, and HAM pH 10 and HAM pH 10δ at 2400 μM (Figure 6). The relation between the microcompound synthesis method and the cytotoxicity of the resulting nanoparticles was dependant on the honey samples used. HSB pH 10 and HSB pH 10δ nanoparticles are more cytotoxic than their HAM counterparts, and HSB pH 10δ was more cytotoxic than HSB pH 10 (Figure 6).

As for the selectivity ratios, the HAM pH 10, HAM pH 10δ, HSB pH 10, and HSB pH 10δ presented the highest values. The cytotoxicity intensity of silver nanoparticles noted in the studies described can be related to many factors. For example, authors such as Akter et al. (2017) [107], Albers et al. (2013) [108] and Gliga et al. (2014) [109] have reported that the cytotoxicity of silver nanoparticles is size-dependent and related to their ion release. In this case, the lower cytotoxicity can be associated with the lower bactericidal effect and high ionic force (which lowers Ag^+ release) described previously [9,14,59].

However, while highest CC50 concentrations were found in pH 10 and pH 10δ among treatments with microcompounds produced with HAM; ML and MLδ were the least among the microcompounds fabricated with HSB. HSB, HSB ML, and HSB MLδ, which are bactericidal at 62.5 μM were the least cytotoxic; as their CC50 of 5283 μM and 4826 μM, respectively, and thus the cell viability rate was higher than 80% even at 1840 μM (or 200 $\mu g \cdot mL^{-1}$). Those microcompounds have larger sizes, as measured by DLS (Table 3), which size can be related to the cytotoxic

Table 9. Washed microcompound concentration necessary to inhibit LLC-MK2 cell by 50% (CC50) and selectivity ratios of treatments.

HAM Microcompound	CC50 (μM)	Microcompound Selectivity index	Washed Microcompound Selectivity index
HAM L	732	11.7	5.9
HAM Lδ	1692	27.1	6.8
HAM pH 5	2726	21.8	10.9
HAM pH 5δ	1021	8.2	8.2
HAM pH 10	>6000	>96.0	>48.0
HAM pH 10δ	>6000	>96.0	>24.0
HSB Microcompound	CC50 (μM)	Microcompound Selectivity index	Washed Microcompound Selectivity index
HSB L	5283	84.5	42.2
HSB Lδ	4826	77.2	38.6
HSB pH 5	1473	23.6	5.9
HSB pH 5δ	1384	22.1	11.1
HSB pH 10	2973	47.6	95.1
HSB pH 10δ	712	11.4	11.4

Notes: The selectivity ratios are defined by dividing the CC50 listed in figures 10A and 10B with either the corresponding microcompound MIC (microcompound selectivity index) or corresponding washed microcompound MIC (washed microcompound selectivity index). Abbreviations: CC50, 50% cytotoxic concentration; Control, LLC-MK2 not submitted to any nanoparticle treatment; HAM, Microcompounds with honey samples collected from *Apis mellifera* honey honeycombs; HSB, Microcompounds with honey samples collected from *Scaptotrigona bipunctata* honeycombs; L, microcompound obtained by light exposure; Lδ, microcompound obtained by light exposure and heating.

effect as it is the case for nanoparticles.

Studies regarding silver nanoparticle toxicity have reported a reduction in cell viability after silver nanoparticles application in concentrations as low as 5 $\mu g \cdot mL^{-1}$, death of human skin epithelial cells at 50 $\mu g \cdot mL^{-1}$ to 100 $\mu g \cdot mL^{-1}$; to compromise human liver cell growth at 5 $\mu g \cdot mL^{-1}$ and to induce apoptosis these cells at 80 $ugmL^{-1}$ [107-112]. Thus, the data indicate that the use of nanoparticles in microcompounds might be a safer alternative. This finding is further grounded in other works showing associations between nanoparticles and other materials to reduce the nanoparticle concentration necessary for a bactericidal effect and thus high selectivity ratios [113,114].

4. Conclusions

In summary, silver microcompounds presented different characteristics due to the honey sample, method of biogenic synthesis used and application of a heat treatment. They presented similar Minimal Inhibitory Concentrations similar to smaller nanoparticles and much lower than concentrations found cytotoxic in our studies, as well as in literature [67-77,84-88,107-112]. Most microcompounds demonstrated themselves to be effective bactericidal agents at 125 μM. In particular, HSB microcompounds synthetized using sunlight were shown to have a selective bactericidal effect; while HAM microcompounds obtained by basification to pH 10 presented the capacity to control bacterial growth while not reducing mammalian cell viability at 2400 μM, which might be related to the excessive aggregation in highly alkaline solutions [9,14,59]. Additionally, our analysis has shown that there are many factors involved between the synthesis of microcompounds with honey and their application against bacterial infections; from the composition of the honey chosen to the target bacterial strain, which can impact the optimization of their usage. Nonetheless, as it is shown by investigating the results gathered with the current literature, there is much potential in the use of the antibacterial properties of silver microcompounds.

Author Contributions

Victor Hugo Clébis: Writing, methodology, data analysis and article analysis. Gerson Nakazato: data analysis and article analysis. Renata Kobaishi: data analysis and article analysis. Sara Scandoriero: data analysis and article analysis. Wilma Aparecida Spinosa: Methodology (honey analysis). Viviane Lopes Leite da Costa: Methodology (honey analysis). Isabella Martins Lourenço: Methodology (dynamic light scattering). Amedea Barozzi Seabrac,: Methodology (dynamic light scattering).

Conflict of Interest

There is no conflict of interest.

References

[1] O'Neill, J., 2020. Tackling drug-resistant infections globally: final report and recommendations. Review on Antimicrobial Resistance website. May 19, 2016. Available from: http://www.pewinternet.org/Presentations/2009/40-The-rise-of-the-e-patient.aspx. (Accessed July 13, 2020)

[2] European Centre for Disease prevention and Control, 2017. Antimicrobial resistance surveillance in Europe 2015. Annual Report Of The European Antimicrobial Resistance Surveillance Network (EARS-Net). Stockholm: ECDC.

[3] World Health Organization, 2017. Prioritization of pathogens to guide discovery, research and development of new antibiotics for drug-resistant bacterial infections, including tuberculosis. License WHO/EMP/IAU/2017.12. Available from: https://apps.who.int/iris/handle/10665/311820?locale-attribute=pt&. (Accessed September 25, 2020)

[4] Interagency Coordination Group on Antimicrobial Resistance, 2019. No time to wait: Securing the future from drug-resistant infections. World Health Organization website. Available from: https://www.who.int/publications/i/item/no-time-to-wait-securing-the-future-from-drug-resistant-infections. (Accessed September 25, 2020)

[5] The Pew Charitable Trusts, 2016. A scientific roadmap for antibiotic discovery. The Pew Research Charitable Trusts website. Available from: https://www.pewtrusts.org/-/media/assets/2016/05/ascientificroadmapforantibioticdiscovery.pdf. (Accessed September 25, 2020)

[6] Lemire, J., Harrison, J., Turner, R., 2013. Antimicrobial activity of metals: mechanisms, molecular targets and applications. Nature Reviews Microbiology. 11(6), 371-384.
DOI: https://doi.org/10.1038/nrmicro3028

[7] Chernousova, S., Epple, M., 2012. Silver as Antibacterial Agent: Ion, Nanoparticle, and Metal. Angewandte Chemie International Edition. 52(6), 1636-1653.
DOI: https://doi.org/10.1002/anie.201205923

[8] Kim, J., Kuk, E., Yu, K., et al., 2007. Antimicrobial effects of silver nanoparticles. Nanomedicine. 3(1), 95-101.
DOI: https://doi.org/10.1016/j.nano.2006.12.001

[9] Wang, R., Neoh, K., Kang, E., et al., 2014. Antifouling coating with controllable and sustained silver release for long-term inhibition of infection and encrustation in urinary catheters. Journal of Biomedical Materials Research. 103(3), 519-528.
DOI: https://doi.org/10.1002/jbm.b.33230

[10] Gibson, D.J., Yang, Q., Kerekes, D.T., et al., 2014. Medical Honey and Silver Dressings Do Not Interfere with Each Other's Key Functional Attributes. Wounds. 26(11), 309-316.

[11] Gupta, A., Mumtaz, S., Li, C., et al., 2019. Combatting antibiotic-resistant bacteria using nanomaterials. Chemical Society Reviews. 48(2), 415-427.
DOI: https://doi.org/10.1039/c7cs00748e

[12] Gupta, A., Landis, R., Rotello, V., 2016. Nanoparticle-based antimicrobials: Surface functionality is critical. F1000Res. 5, 364.
DOI: https://doi.org/10.12688/f1000research.7595.1

[13] Neu, H., 1992. The crisis in antibiotic resistance. Science. 257(5073), 1064-1073.
DOI: https://doi.org/10.1126/science.257.5073.1064

[14] Wang, L., Hu, C., Shao, L., 2017. The antimicrobial activity of nanoparticles: present situation and prospects for the future. International Journal of Nanomedicine. 12, 1227-1249.
DOI: https://doi.org/10.2147/ijn.s121956

[15] Zhao, Y., Tian, Y., Cui, Y., et al., 2010. Small molecule-capped gold nanoparticles as potent antibacterial agents that target gram-negative bacteria. Journal of the American Chemical Society. 132(35), 12349-12356.
DOI: https://doi.org/10.1021/ja1028843

[16] Fortas, W., Djelad, A., Dib-Bellahouel, S., et al., 2022. Ionic liquid-functionalised AlPO-34 material prepared by ionothermal method for efficient antibacterial property against Escherichia coli. Materials Research Innovations.
DOI: https://doi.org/10.1080/14328917.2022.2095840

[17] Zhou, Q., Wang, T., Wang, C., et al., 2020. Synthesis and characterization of silver nanoparticles-doped hydroxyapatite/alginate microparticles with promising cytocompatibility and antibacterial properties. Colloids and Surfaces A: Physicochemical and Engineering Aspects. 585, 124081.
DOI: https://doi.org/10.1016/j.colsurfa.2019.124081

[18] Balasooriya, E., Jayasinghe, C., Jayawardena, U., et al., 2017. Honey mediated green synthesis of nanoparticles: New era of safe nanotechnology. Journal of Nanomaterials. 1-10.
DOI: https://doi.org/10.1155/2017/5919836

[19] El-Desouky, T., Ammar, H., 2016. Honey mediated silver nanoparticles and their inhibitory effect on

aflatoxins and ochratoxin A. Journal of Applied Pharmaceutical Science. 6(6), 83-90.
DOI: https://doi.org/10.7324/japs.2016.60615

[20] González Fá, A., Juan, A., Di Nezio, M., 2016. Synthesis and characterization of silver nanoparticles prepared with honey: The role of carbohydrates. Analytical Letters. 50(5), 877-888.
DOI: https://doi.org/10.1080/00032719.2016.1199558

[21] Mittal, A., Chisti, Y., Banerjee, U., 2013. Synthesis of metallic nanoparticles using plant extracts. Biotechnology Advances. 31(2), 346-356.
DOI: https://doi.org/10.1016/j.biotechadv.2013.01.003

[22] González-Miret, M., Terrab, A., Hernanz, D., et al., 2005. Multivariate correlation between color and mineral composition of honeys and by their botanical origin. Journal of Agricultural and Food Chemistry. 53(7), 2574-2580.
DOI: https://doi.org/10.1021/jf048207p

[23] Bar, H., Bhui, D., Sahoo, G., et al., 2009. Green synthesis of silver nanoparticles using seed extract of Jatropha curcas. Colloids and Surfaces A: Physicochemical and Engineering Aspects. 348(1-3), 212-216.
DOI: https://doi.org/10.1016/j.colsurfa.2009.07.021

[24] Olaitan, P.B., Adeleke, O.E., Ola, I.O., 2007. Honey: a reservoir for microorganisms and an inhibitory agent for microbes. African Health Sciences. 7(3), 159-165.
DOI: https://doi.org/10.5555/afhs.2007.7.3.159

[25] Obot, I., Umoren, S., Johnson, A., 2013. Sunlight-mediated synthesis of silver nanoparticles using honey and its promising anticorrosion potentials for mild steel in acidic environments. JMES. 4(6), 1013-1018. https://www.academia.edu/6634621/Sunlight-mediated_synthesis_of_silver_nanoparticles_using_honey_and_its_promising_anticorrosion_potentials_for_mild_steel_in_acidic_environments. (Accessed September 25, 2020)

[26] Philip, D., 2009. Honey mediated green synthesis of gold nanoparticles. Spectrochimica Acta Part A: Molecular and Biomolecular Spectroscopy. 73(4), 650-653.
DOI: https://doi.org/10.1016/j.saa.2009.03.007

[27] Philip, D., 2010. Honey mediated green synthesis of silver nanoparticles. Spectrochimica Acta Part A: Molecular and Biomolecular Spectroscopy. 75(3), 1078-1081.
DOI: https://doi.org/10.1016/j.saa.2009.12.058

[28] Madhu, G., Kumar, A., Nair, S., 2019. Sunlight-induced honey-mediated green synthesis of silver nanoparticles. AIP Conference Proceedings. 2162(1).
DOI: https://doi.org/10.1063/1.5130311

[29] Kwakman, P., Velde, A., Boer, L., et al., 2010. How honey kills bacteria. FASEB Journal. 24(7), 2576-2582.
DOI: https://doi.org/10.1096/fj.09-150789

[30] Kwakman, P., Zaat, S., 2011. Antibacterial components of honey. IUBMB Life. 64(1), 48-55.
DOI: https://doi.org/10.1002/iub.578

[31] Cortopassi-Laurino, M., Gelli, D., 1991. Pollen analysis, physico-chemical properties and antibacterial action of Brazilian honeys from Africanized honeybees (Apis mellifera L) and stingless bees. Apidologie (Celle). 22(1), 61-73.
DOI: https://doi.org/10.1051/apido:19910108

[32] Poli, J., Guinoiseau, E., Luciani, A., et al., 2018. Investigating the antibacterial action of Corsican honeys on nosocomial and foodborne pathogens. Journal of Apicultural Research. 57(1), 186-194.
DOI: https://doi.org/10.1080/00218839.2017.1412564

[33] Al-Mamary, M., Al-Meeri, A., Al-Habori, M., 2002. Antioxidant activities and total phenolics of different types of honey. Nutrition Research. 22(9), 1041-1047.
DOI: https://doi.org/10.1016/s0271-5317(02)00406-2

[34] Alves, R., Souza, B., Carvalho, C., et al., 2005. Cost of honey production: A proposal for africanized bees and meliponines. 1st ed. Cruz das Almas: Universidade Federal da Bahia/SEAGRI-BA.

[35] Bueno-Costa, F., Zambiazi, R., Bohmer, B., et al., 2016. Antibacterial and antioxidant activity of honeys from the state of Rio Grande do Sul, Brazil. LWT. 65, 333-340.
DOI: https://doi.org/10.1016/j.lwt.2015.08.018

[36] Clébis, V., Nishio, E., Scandorieiro, S., et al., 2019. Antibacterial effect and clinical potential of honey collected from *Scaptotrigona bipunctata* Lepeletier (1836) and Africanized bees *Apis mellifera* Latreille and their mixture. Journal of Apicultural Research. 1-11.
DOI: https://doi.org/10.1080/00218839.2019.1681118

[37] Cushnie, T., Lamb, A., 2006. Errata for "Antimicrobial activity of flavonoids". International Journal of Antimicrobial Agents. 27(2), 181.
DOI: https://doi.org/10.1016/j.ijantimicag.2005.12.002

[38] Nishio, E., Ribeiro, J., Oliveira, A., et al., 2016. Antibacterial synergic effect of honey from two stingless bees: *Scaptotrigona bipunctata* Lepeletier, 1836, and *S. postica* Latreille, 1807. Scientific Reports. 6(1).
DOI: https://doi.org/10.1038/srep21641

[39] Adams, C., Manley-Harris, M., Molan, P., 2009. The origin of methylglyoxal in New Zealand manuka

(*Leptospermum scoparium*) honey. Carbohydrate Research. 344(8), 1050-1053.
DOI: https://doi.org/10.1016/j.carres.2009.03.020

[40] Molan, P., Betts, J., 2004. Clinical usage of honey as a wound dressing: an update. Journal of Wound Care. 13(9), 353-356.
DOI: https://doi.org/10.12968/jowc.2004.13.9.26708

[41] Latimer, G., 2019. Official methods of analysis of AOAC International. 21st ed. Gaithersburg, Maryland: AOAC International.

[42] Priz, M., 2014. Influence of Different Parameters on Wet Synthesis of Silver. (bachelor's thesis). Enschede, NL: University of Twente.

[43] Tagad, C., Dugasani, S., Aiyer, R., et al., 2013. Green synthesis of silver nanoparticles and their application for the development of optical fiber based hydrogen peroxide sensor. Sensors and Actuators B:Chemical. 183, 144-149.
DOI: https://doi.org/10.1016/j.snb.2013.03.106

[44] Patel, K., Deshpande, M., Gujarati, V., et al., 2016. Effect of heating time duration on synthesis of colloidal silver nanoparticles. Advanced Materials. 1141, 14-18.
DOI: https://doi.org/10.4028/www.scientific.net/amr.1141.14

[45] Clinical & Laboratory Standards Institute (CLSI), 2018. Methods for dilution antimicrobial susceptibility tests for bacteria that grow aerobically. 11th ed. CLSI standard M07. Wayne, PA: Clinical and Laboratory Standards Institute.

[46] Clébis, V., Proni, E., Sarimento, J.P., et al., 2021. Antibacterial activity of silver microparticles encapsulated with honeys from *Apis mellifera* and *Scaptotrigona bipunctata*. Brazilian Journal Of Animal And Environmental Research. 4(1), 933-948.
DOI: https://doi.org/10.34188/bjaerv4n1-076

[47] National Committee for Clinical Laboratory Standards (NCCLS), 1999. Methods for determining bactericidal activity of antimicrobial agents: Approved guideline. Wayne (Pennsylvania): NCCLS.

[48] El-Desouky, T., Ammar, H., 2016. Honey mediated silver nanoparticles and their inhibitory effect on aflatoxins and ochratoxin A. Journal of Pharmaceutical Sciences. 6(6), 83-90.
DOI: https://doi.org/10.7324/japs.2016.60615

[49] Haiza, H., Azizan, A., Mohidin, A., et al., 2013. Green synthesis of silver nanoparticles using local honey. NH. 4, 87-98.
DOI: https://doi.org/10.4028/www.scientific.net/nh.4.87

[50] Raveendran, P., Fu, J., Wallen, S., 2006. A simple and "green" method for the synthesis of Au, Ag, and Au–Ag alloy nanoparticles. Green Chemistry. 8(1), 34-38.
DOI: https://doi.org/10.1039/b512540e

[51] Meshram, S., Bonde, S., Gupta, I., et al., 2013. Green synthesis of silver nanoparticles using white sugar. IET Nanobiotechnology. 7(1), 28-32.
DOI: https://doi.org/10.1049/iet-nbt.2012.0002

[52] Catauro, M., Tranquillo, E., Dal Poggetto, G., et al., 2018. Influence of the heat treatment on the particles size and on the crystalline phase of TiO_2 synthesized by the sol-gel method. Materials (Basel). 11(12), 2364.
DOI: https://doi.org/10.3390/ma11122364

[53] Granbohm, H., Larismaa, J., Ali, S., et al., 2018. Control of the size of silver nanoparticles and release of silver in heat treated SiO_2-Ag composite powders. Materials (Basel). 11(1), 80.
DOI: https://doi.org/10.3390/ma11010080

[54] Jiang, X.C., Chen, W.M., Chen, C.Y., et al., 2011. Role of temperature in the growth of silver nanoparticles through a synergetic reduction approach. Nanoscale Research Letters. 6(1), 32.
DOI: https://doi.org/10.1007/s11671-010-9780-1

[55] Barrett, K., Barman, S., Yuan, J., et al., 2019. Ganong's Review Of Medical Physiology. 26th ed. New York, N.Y.: McGraw-Hill Education LLC.

[56] Radovic-Moreno, A., Lu, T., Puscasu, V., et al., 2012. Surface charge-switching polymeric nanoparticles for bacterial cell wall-targeted delivery of antibiotics. ACS Nano. 6(5), 4279-4287.
DOI: https://doi.org/10.1021/nn3008383

[57] Zinni, Y., 2020. Types of microorganisms & optimum pH. Sciencing. https://sciencing.com/types-microorganisms-optimum-ph-8618232.html. (Accessed July 14, 2020)

[58] Qiao, Z., Yao, Y., Song, S., et al., 2019. Silver nanoparticles with pH induced surface charge switchable properties for antibacterial and antibiofilm applications. Journal of Materials Chemistry B. 7(5), 830-840.
DOI: https://doi.org/10.1039/c8tb02917b

[59] Abbaszadegan, A., Ghahramani, Y., Gholami, A., et al., 2015. The effect of charge at the surface of silver nanoparticles on antimicrobial activity against gram-positive and gram-negative bacteria: A preliminary study. Journal of Nanomaterials. 1-8.
DOI: https://doi.org/10.1155/2015/720654

[60] Official Journal of the European Union, 2011. Commission recommendation on the definition of nanomaterial (text with EEA relevance*)*. Retrieved from: https://eur-lex.europa.eu/eli/reco/2011/696/oj. (Ac-

cessed September 25, 2020)

[61] Food and Drug Administration, 2014. Considering whether an FDA-regulated product involves the application of nanotechnology. Retrieved from: https://www.fda.gov/regulatory-information/search-fda-guidance-documents/considering-whether-fda-regulated-product-involves-application-nanotechnology. (Accessed September 25, 2020)

[62] Santamarina, J., Cho, G., 2004. Soil behaviour: The role of particle shape. Jardine R, Potts D, Higgins K, ed. Soil Advances In Geotechnical Engineering: The Skempton Conference. 1st ed. London: Thomas Telford. 604-617. https://www.icevirtuallibrary.com/doi/abs/10.1680/aigev1.32644.0035. (Accessed September 25, 2020)
DOI: https://doi.org/10.1680/aigev1.32644.0035

[63] Berrezueta, E., Cuervas-Mons, J., Rodríguez-Rey, Á., et al., 2019. Representativity of 2D Shape Parameters for Mineral Particles in Quantitative Petrography. Minerals. 9(12), 768.
DOI: https://doi.org/10.3390/min9120768

[64] Helmlinger, J., Sengstock, C., Groß-Heitfeld, C., et al., 2016. Silver nanoparticles with different size and shape: equal cytotoxicity, but different antibacterial effects. RSC Advances. 6(22), 18490-18501.
DOI: https://doi.org/10.1039/c5ra27836h

[65] Pal, S., Tak, Y., Song, J., 2007. Does the Antibacterial Activity of Silver Nanoparticles Depend on the Shape of the Nanoparticle? A Study of the Gram-Negative Bacterium Escherichia coli. Applied And Environmental Microbiology. 73(6), 1712-1720.
DOI: https://doi.org/10.1128/aem.02218-06

[66] Cheon, J., Kim, S., Rhee, Y., et al., 2019. Shape-dependent antimicrobial activities of silver nanoparticles. International Journal of Nanomedicine. 14, 2773-2780.
DOI: https://doi.org/10.2147/IJN.S196472

[67] Escárcega-González, C., Garza-Cervantes, J., Vazquez-Rodríguez, A., et al., 2018. *In vivo* antimicrobial activity of silver nanoparticles produced via a green chemistry synthesis using *Acacia rigidula* as a reducing and capping agent. International Journal of Nanomedicine. 13, 2349-2363.
DOI: https://doi.org/10.2147/ijn.s160605

[68] Fayaz, A., Balaji, K., Girilal, M., et al., 2010. Biogenic synthesis of silver nanoparticles and their synergistic effect with antibiotics: a study against gram-positive and gram-negative bacteria. Nanomedicine: NBM. 6(1), 103-109.
DOI: https://doi.org/10.1016/j.nano.2009.04.006

[69] Hajipour, M., Fromm, K., Akbar Ashkarran, A., et al., 2012. Antibacterial properties of nanoparticles. Trends Biotechnol. 30(10), 499-511.
DOI: https://doi.org/10.1016/j.tibtech.2012.06.004

[70] Khan, A., 2012. Medicine at nanoscale: a new horizon. International Journal of Nanomedicine. 7, 2997-2998.
DOI: https://doi.org/10.2147/IJN.S33238

[71] Khan, S., Mukherjee, A., Chandrasekaran, N., 2011. Studies on interaction of colloidal silver nanoparticles (SNPs) with five different bacterial species. Colloids and Surfaces B-Biointerfaces. 87(1), 129-138.
DOI: https://doi.org/10.1016/j.colsurfb.2011.05.012

[72] Leid, J., Ditto, A., Knapp, A., et al., 2011. In vitro antimicrobial studies of silver carbene complexes: activity of free and nanoparticle carbene formulations against clinical isolates of pathogenic bacteria. Journal of Antimicrobial Chemotherapy. 67(1), 138-148.
DOI: https://doi.org/10.1093/jac/dkr408

[73] Morones, J., Elechiguerra, J., Camacho, A., et al., 2005. The bactericidal effect of silver nanoparticles. Nanotechnology. 16(10), 2346-2353.
DOI: https://doi.org/10.1088/0957-4484/16/10/059

[74] Qais, F., Shafiq, A., Khan, H., et al., 2019. Antibacterial effect of silver nanoparticles synthesized using *Murraya koenigii* (L.) against multidrug-resistant pathogens. Bioinorganic Chemistry and Applications. 1-11.
DOI: https://doi.org/10.1155/2019/4649506

[75] Sinha, R., Karan, R., Sinha, A., et al., 2011. Interaction and nanotoxic effect of ZnO and Ag nanoparticles on mesophilic and halophilic bacterial cells. Bioresource Technology. 102(2), 1516-1520.
DOI: https://doi.org/10.1016/j.biortech.2010.07.117

[76] Sreelakshmi, C., Datta, K., Yadav, J., et al., 2011. Honey Derivatized Au and Ag Nanoparticles and Evaluation of Its Antimicrobial Activity. Journal of Nanoscience and Nanotechnology. 11(8), 6995-7000.
DOI: https://doi.org/10.1166/jnn.2011.4240

[77] Ashkarran, A., Ghavami, M., Aghaverdi, H., et al., 2012. Bacterial Effects and Protein Corona Evaluations: Crucial Ignored Factors in the Prediction of Bio-Efficacy of Various Forms of Silver Nanoparticles. Chemical Research in Toxicology. 25(6), 1231-1242.
DOI: https://doi.org/10.1021/tx300083s

[78] Brudzynski, K., 2020. A current perspective on hydrogen peroxide production in honey. A review. Food Chemistry. 332, 127229.
DOI: https://doi.org/10.1016/j.foodchem.2020.127229

[79] Baek, Y., An, Y., 2011. Microbial toxicity of metal

oxide nanoparticles (CuO, NiO, ZnO, and Sb2O3) to *Escherichia coli, Bacillus subtilis*, and *Streptococcus aureus*. Science of the Total Environment. 409(8), 1603-1608.
DOI: https://doi.org/10.1016/j.scitotenv.2011.01.014

[80] Lagbas, A., Pelisco, J., Riego, V., 2016. Antibacterial activity of silver nano/microparticles in chitosan matrix prepared using *Mangifera indica* and *Chrysophyllum cainito* leaf extracts and its application in pineapple (*Ananas comosus*) polyester fabric. IJACS. 4(1), 7-13.
DOI: https://doi.org/10.1016/j.colsurfb.2011.05.012

[81] Gupta, A., Mumtaz, S., Li, C., et al., 2019. Combatting antibiotic-resistant bacteria using nanomaterials. Chemical Society Reviews. 48(2), 415-427.
DOI: https://doi.org/10.1039/c7cs00748e

[82] Jimenez, M., Beristain, C., Azuara, E., et al., 2016. Physicochemical and antioxidant properties of honey from *Scaptotrigona mexicana* bee. Journal of Apicultural Research. 55(2), 151-160.
DOI: https://doi.org/10.1080/00218839.2016.1205294

[83] Rani, G., Narasinga Rao, B., Shamilli, M., et al., 2018. Combined effect of silver nanoparticles and honey in experimental wound healing process in rats. BioMed Research International. 29(15), 3074-3078.
DOI: https://doi.org/10.4066/biomedicalresearch. 29-18-898

[84] Mohamed, D.S., Abd El-Baky, R.M., Sandle, T., et al., 2020. Antimicrobial activity of silver-treated bacteria against other multi-drug resistant pathogens in their environment. Antibiotics (Basel). 9(4), 181.
DOI: https://doi.org/10.3390/antibiotics9040181

[85] Loo, Y.Y., Rukayadi, Y., Nor-Khaizura, M.A., et al., 2018. *In vitro* antimicrobial activity of green synthesized silver nanoparticles against Selected Gram-negative foodborne Pathogens. Front Microbiol. 9, 1555.
DOI: https://doi.org/10.3389/fmicb.2018.01555

[86] Das B et al., 2017. Green synthetized silver nanoparticles destroy multidrug resistant bacteria via reactive oxygen species mediated membrane damage. Arabian Journal of Chemistry. 10(6), 862-876.
DOI: https://doi.org/10.1016/j.arabjc.2015.08.008

[87] Abdelsattar, A.S., Hakim, T.A., Rezk, N., et al., 2022. Green synthesis of silver nanoparticles using Ocimum basilicum L. and Hibiscus sabdariffa L. extracts and their antibacterial activity in combination with phage ZCSE6 and sensing properties. Journal of Inorganic and Organometallic Polymers. 32, 1951-1965.
DOI: https://doi.org/10.1007/s10904-022-02234-y

[88] Amin, M., et al., 2014. Green synthesis of silver nanoparticles: Strucutural features and *in vivo* and *in vitro* therapeutic effects against *Heliobacter pylori* induced gastritis. Bioinorganic Chemistry and Applications. 4, 1-11.
DOI: https://doi.org/10.1155/2014/135824

[89] Cushnie, T., O'Driscoll, N., Lamb, A., 2016. Morphological and ultrastructural changes in bacterial cells as an indicator of antibacterial mechanism of action. Cellular And Molecular Life Sciences. 73(23), 4471-4492.
DOI: https://doi.org/10.1007/s00018-016-2302-2

[90] Klainer, A.S., Perkins, R.L., 1972. Surface manifestations of antibiotic-induce alterations in protein synthesis in bacterial cells. Antimicrob Agents Chemother. 1(2), 164-170.
DOI: https://doi.org/10.1128/aac.1.2.164

[91] Thammawithan, S., Siritongsuk, P., Nasompag, S., et al., 2021. A Biological Study of Anisotropic Silver Nanoparticles and Their Antimicrobial Application for Topical Use. Journal of Veterinary Science. 8(9), 177.
DOI: https://doi.org/10.3390/vetsci8090177

[92] Boberek, J., Stach, J., Good, L., 2010. Genetic evidence for inhibition of bacterial division protein FtsZ by berberine. PLoS One. 5(10), e13745.
DOI: https://doi.org/10.1371/journal.pone.0013745

[93] Radman, M., 1975. SOS repair hypothesis: phenomenology of an inducible DNA repair which is accompanied by mutagenesis. Basic Life Sciences. 5A, 355-367.
DOI: https://doi.org/10.1007/978-1-4684-2895-7_48

[94] Spratt, B.G., 1975. Distinct penicillin binding proteins involved in the division, elongation, and shape of *Escherichia coli* K12. Proceedings of the National Academy of Sciences of the United States of America. 72(8), 2999-3003.
DOI: https://doi.org/10.1073/pnas.72.8.2999

[95] Toyofuku, M., Nomura, N., Eberl, L., 2019. Types and origins of bacterial membrane vesicles. Nature Reviews Microbiology. 17(1), 13-24.
DOI: https://doi.org/10.1038/s41579-018-0112-2

[96] Lee, W., Kim, K.J., Lee, D.G., 2014. A novel mechanism for the antibacterial effect of silver nanoparticles on *Escherichia coli*. Biometals. 27(6), 1191-1201.
DOI: https://doi.org/10.1007/s10534-014-9782-z

[97] Dwyer, D.J., Camacho, D.M., Kohanski, M.A., et al., 2012. Antibiotic-induced bacterial cell death exhibits physiological and biochemical hallmarks of apoptosis. Molecular Cell. 46(5), 561-572.
DOI: https://doi.org/10.1016/j.molcel.2012.04.027

[98] Rai, M., Yadav, A., Gade, A., 2009. Silver nanoparticles as a new generation of antimicrobials. Biotechnology Advances. 27(1), 76-83.
DOI: https://doi.org/10.1016/j.biotechadv.2008.09.002.

[99] Li, W.R., Xie, X.B., Shi, Q.S., et al., 2010. Antibacterial activity and mechanism of silver nanoparticles on *Escherichia coli*. Applied Microbiology and Biotechnology. 85(4), 1115-1122.
DOI: https://doi.org/10.1007/s00253-009-2159-5

[100] Brudzynski, K., Sjaarda, C., 2014. Antibacterial compounds of Canadian honeys target bacterial cell wall inducing phenotype changes, growth inhibition and cell lysis that resemble action of β-lactam antibiotics. PLoS One. 9(9), e106967.
DOI: https://doi.org/10.1371/journal.pone.0106967

[101] Elliott, T.S., Rodgers, F.G., 1985. Morphological response and growth characteristics of *Legionella pneumophila* exposed to ampicillin and erythromycin. Journal of Medical Microbiology. 19(3), 383-390.
DOI: https://doi.org/10.1099/00222615-19-3-383

[102] Tsang, K.W., Ng, P., Ho, P.L., et al., 2003. Effects of erythromycin on *Pseudomonas aeruginosa* adherence to collagen and morphology in vitro. European Respiratory Journal. 21(3), 401-406.
DOI: https://doi.org/10.1183/09031936.03.00050903

[103] Burdett, I.D., Murray, R.G., 1974. Septum formation in *Escherichia coli*: characterization of septal structure and the effects of antibiotics on cell division. Journal of Bacteriology. 119(1), 303-324.
DOI: https://doi.org/10.1128/JB.119.1.303-324.1974

[104] Siddique, M., Aslam, B., Imran, M., et al., 2020. Effect of Silver Nanoparticles on Biofilm Formation and EPS Production of Multidrug-Resistant *Klebsiella pneumoniae*. Biomed Research International. 1-9.
DOI: https://doi.org/10.1155/2020/6398165

[105] Sadeghi-Aliabadi, H., Hamzeh, J., Mirian, M., 2015. Investigation of Astragalus honey and propolis extract's cytotoxic effect on two human cancer cell lines and their oncogen and proapoptotic gene expression profiles. Advanced NanoBiomed Research. 4(42).
DOI: https://doi.org/10.4103/2277-9175.151251

[106] Milić, M., Leitinger, G., Pavičić, I., et al., 2015. Cellular uptake and toxicity effects of silver nanoparticles in mammalian kidney cells. Journal of Applied Toxicology. 35(6), 581-592.
DOI: https://doi.org/10.1002/jat.3081

[107] Akter, M., Sikder, M.T., Rahman, M.M., et al., 2017. A systematic review on silver nanoparticles-induced cytotoxicity: Physicochemical properties and perspectives. Journal of Advanced Research. 9, 1-16.
DOI: https://doi.org/10.1016/j.jare.2017.10.008

[108] Albers, C.E., Hofstetter, W., Siebenrock, K.A., et al., 2013. In vitro cytotoxicity of silver nanoparticles on osteoblasts and osteoclasts at antibacterial concentrations. Nanotoxicology. 7(1), 30-36.
DOI: https://doi.org/10.3109/17435390.2011.626538

[109] Gliga, A.R., Skoglund, S., Wallinder, I.O., et al., 2014. Size-dependent cytotoxicity of silver nanoparticles in human lung cells: the role of cellular uptake, agglomeration and Ag release. Part Fibre Toxicol. 11, 11.
DOI: https://doi.org/10.1186/1743-8977-11-11

[110] Kaur, J., Tikoo, K., 2013. Evaluating cell specific cytotoxicity of differentially charged silver nanoparticles. Food And Chemical Toxicology. 51, 1-14.
DOI: https://doi.org/10.1016/j.fct.2012.08.044

[111] Liu, P., Guan, R., Ye, X., et al., 2011. Toxicity of nano- and micro-sized silver particles in human hepatocyte cell line L02. Journal of Physics: Conference Series. 304, 012036.
DOI: https://doi.org/10.1088/1742-6596/304/1/012036

[112] Jiao, Z.H., Li, M., Feng, Y.X., et al., 2014. Hormesis effects of silver nanoparticles at non-cytotoxic doses to human hepatoma cells. PLoS One. 9(7), e102564.
DOI: https://doi.org/10.1371/journal.pone.0102564

[113] Lima, D.S., Gullon, B., Cardelle-Cobas, A., et al., 2017. Chitosan-based silver nanoparticles: A study of the antibacterial, antileishmanial and cytotoxic effects. Journal of Bioactive and Bompatible Polymers. 32(4), 397-410.
DOI: https://doi.org/10.1177/0883911516681329

[114] Figueiredo, E.P., Ribeiro, J.M., Nishio, E.K., et al., 2019. New Approach For Simvastatin As An Antibacterial: Synergistic Effect With Bio-Synthesized Silver Nanoparticles Against Multidrug-Resistant Bacteria. International Journal of Nanomedicine. 14, 7975-7985.
DOI: https://doi.org/10.2147/IJN.S211756